SIAM J. MATH. ANAL.
Vol. 28, No. 6, pp. 1457–1489, November 1997

011

DYNAMICS AND CONDENSATION OF COMPLEX SINGULARITIES FOR BURGERS' EQUATION I*

DAVID SENOUF†

Dedicated to Sophia de Rosnay

Abstract. Spatial analyticity properties of the solution to Burgers' equation with a generic initial data are presented, following the work of Bessis and Fournier [*Research Reports in Physics: Nonlinear Physics*, Springer-Verlag, Berlin, Heidelberg, 1990, pp. 252–257]. The positive viscosity solution is a meromorphic function with a countable set of conjugate poles confined to the imaginary axis. Their motion is governed by an infinite-dimensional Calogero dynamical system (CDS). The inviscid solution is a three-sheeted Riemann surface with three branch-point singularities.

Exact pole locations are found independent of the viscosity at the inviscid shock time t_*. For $t \neq t_*$, the time evolution of the poles is obtained numerically by solving a truncated version of the CDS. A Runge–Kutta scheme is used together with a "multipole" algorithm to deal with the computationally intensive nonlinear interaction of the poles. Additionally, for $t \leq t_*$, the small viscosity behavior of the poles is shown to be a perturbation of the conjugate inviscid branch-point singularities $\pm x_s(t)$. The numerical pole dynamics also provide the width of the analyticity strip which remains uniformly bounded away from zero, agreeing with asymptotic predictions.

For small $\nu > 0$ and $t \geq t_*$, different saddle-point approximations of the solution are found within and outside the caustics $x = \pm x_s(t)$. The transition between the two regimes at $x = \pm x_s(t)$ is described by a uniform asymptotic expansion involving the Pearcey integral. The solution is computed for small viscosity using pole dynamics, finite differences (method of lines), and asymptotic methods (saddle-point method); numerical agreement is established.

Key words. partial differential equations, asymptotic approximations, pole dynamics, domain of analyticity

AMS subject classifications. 35A20, 35A40, 35B40, 35Q53, 41A60

PII. S0036141095289373

1. Introduction.

In this article we investigate the spatial analyticity properties of a solution to Burgers' equation (hereafter referred to as "BE"):

$$\frac{\partial u}{\partial t} + u\,\frac{\partial u}{\partial x} = \nu\,\frac{\partial^2 u}{\partial x^2}, \qquad x \in \mathbb{R},\ t > 0,\ \nu \geq 0, \tag{1.1}$$

where the parameter ν is a viscosity coefficient and $u = u_\nu(x,t)$ represents the velocity field of a fluid particle at position x in space and time t. BE is a model for the statistical theory of turbulence [9, 10] which can be thought of as a simplified one-dimensional scalar analog of the Navier–Stokes equations of fluid dynamics. Although it does not exhibit the complexity of the Navier–Stokes equations, it does illustrate the interaction between a nonlinear first-order convective term and a second-order diffusive one. This feature, which is shared with the Navier–Stokes equations, may help us to understand the questions of regularity of so complicated a system. Although Burgers' model is not a good model for turbulence because it does not exhibit any chaotic behavior, there are other important applications besides the Ising model

*Received by the editors July 24, 1995; accepted for publication (in revised form) June 25, 1996. This research was partially supported by NSF grant DMS-9306720.
http://www.siam.org/journals/sima/28-6/28937.html
†Lehman Brothers, One Broadgate, London EC2M 7HA, United Kingdom (dsenouf@lehman.com).

analogy presented by Bessis and Fournier in [7]. A partial list of such applications can be found in the introduction of the work by She, Aurell, and Frisch in [30].

There are many tools which can be used to evaluate domains of analyticity of solutions to nonlinear PDEs: Painlevé expansions, Padé approximants, pole dynamics, spectral methods, the abstract Cauchy–Kowalewski theorem, and, more generally, methods involving analytic norms.

The work of Bardos and Benachour [5] was pioneering because it used complex analytic techniques (analytic norms) to describe domains of regularity for equations of fluid dynamics: Bardos and Benachour showed that the loss of analyticity for the incompressible Euler equations in $\mathbb{R}^n$ follows from a blowup in the vorticity $\omega = \nabla \times u$, in analogy with the blowup of the solution of the inviscid BE ($\nu = 0$), which is driven by the blowup of the gradient of the solution $\partial u/\partial x$.

Another method which also involves analytic norms is the abstract Cauchy–Kowalewski theorem. A concise and improved version of the original work of Nirenberg [27] can be found in [11]. One of the limitations of this method is that it cannot deal with parabolic PDEs. An interesting combination of Painlevé expansions and the abstract Cauchy–Kowalewski theorem applied to BE can be found in [23].

As far as spectral methods are concerned, we only mention the works of Sulem, Sulem, and Frisch [35] and Fournier and Frisch [19], both of which deal with BE. Reference [35] focuses on the numerical implementation of spectral methods to evaluate the widths of analyticity strips of solutions to nonlinear PDEs. Reference [19] focuses on spectral methods applied to the deterministic and statistical BE. More references can be found in both of these works.

The method of pole dynamics originated with Kruskal's work [26], followed by Calogero [13] and the Choodnovskys [16], who developed a mathematical tool for what was to become a very powerful method to solve nonlinear PDEs. Indeed, they showed that a very large class of nonlinear evolution equations has an associated/equivalent N-body problem/formulation. This method consists in inserting into the PDE a pole expansion of the solution (a Mittag–Leffler expansion where the complex spatial poles are time dependent). Compatibility conditions are found in the form of a dynamical system for these poles; this dynamical system is referred to as the Calogero dynamical system (CDS for short).

In [20], Frisch and Morf describe complex time singularities for nonlinear PDEs as well as make a first attempt to describe spatial singularities for BE through pole dynamics. In [20, section 4], a list of other references which use pole dynamics can be found. In [19], Fournier and Frisch devoted greater attention to (real time) complex spatial singularities for the inviscid BE from a deterministic and a statistical point of view. In the meantime, Thual, Frisch, and Hénon [36] used pole dynamics to compute the stationary pole distribution and stationary solution of a Sivashinsky-type flame-front propagation pseudo-differential equation. From the work of Fournier and Frisch [19], Bessis and Fournier [6, 7] went on to analyze the spatial analytic properties for both the inviscid and viscous deterministic case using a generic initial data. Kimura [25] has described complex space and time pole positions for the BE with periodic initial data by straightforwardly solving for the roots of the Cole–Hopf variable.

In [6, 7], Bessis and Fournier studied the analytical properties of the solution to the BE with a cubic initial data, namely,

$$u(x,0) = u_0(x) = 4x^3 - x/t_*, \qquad x \in \mathbb{R}, \tag{1.2}$$

and t_* is a fixed positive parameter corresponding to the first blowup time of the

solution to the inviscid equation. This work stemmed from the observation [19] that the large wavenumber asymptotic expansion of the Fourier transform of the inviscid solution was degenerate at the shock time t_*; it was even incorrect beyond t_*. Thus, Bessis and Fournier sought for an explanation using complex analytic methods. They showed that the inviscid shock could be interpreted as a permutation of the two sides of the "physical Riemann sheet." As far as the viscous case is concerned, Bessis and Fournier showed that the poles were confined to the imaginary axis and that they satisfied a CDS. Additionally, they presented a "limiting" pole density which characterized the process of pole condensation as $\nu \to 0^+$.

The inviscid equation $u_t + u\,u_x = 0$ is a simple hyperbolic quasi-linear PDE. Its solution develops a cube root singularity at the origin at the time $t = -(\inf_x u_0'(x))^{-1} > 0$, which, for (1.2), equals t_*. This is known to be a generic singularity for the inviscid BE. It is due to the coalescence at the origin ($x = 0$) of two complex conjugate branch points $\pm x_s(t)$ of order two. Thus, the cubic initial data is considered generic due to the local cube root shape of the shock of the inviscid solution at $t = t_*$ and the associated cube root singularity (for further details, see [32, App. A] and [7, 12, 19]). Another compelling reason for which a cubic polynomial is used is that its solution can be completely analyzed for both $\nu > 0$ and $\nu = 0$, unlike a higher-order polynomial of the form $u_0(x) = 2nx^{2n-1} - x/t_*$ (see [32, App. D]).

For $t > t_*$, the inviscid solution has three real values within the real interval $(-x_s, x_s)$, and in the real complement $(-x_s, x_s)^c$ it has one real value and two complex values (see [32, App. C] and [12]). By extending (for all $t > 0$) the domain of the spatial variable x and the range of the solution u into the complex plane, Bessis and Fournier have shown in [6, 7] that the analytic structure (topology) of the inviscid solution is a three-sheeted Riemann surface with three branch points. One is at infinity, and the other two come down the imaginary axis as a conjugate pair and coalesce at the origin at the shock time t_* to form a third-order branch point. The inviscid shock in the real plane is interpreted as the permutation of the physical Riemann sheets which make up the Riemann surface. More precisely, it appears to be the connecting path between the two sides of the physical Riemann sheet which are separated by nonphysical ones (see [6] for more details).

In this work, we propose to correct and extend the results of Bessis and Fournier in [7] by using complex analytic methods and asymptotic methods (including spectral methods). Most important, we show how to use pole dynamics to determine the evolution of the domain of regularity of the solution to BE. This method can be adapted to a wide range of nonlinear PDEs.

The positive viscosity solution ($\nu > 0$) is a meromorphic function with a countable set of conjugate pairs of simple poles for all $t > 0$. These poles move towards the origin along the imaginary axis, then turn around after a finite time and start moving away from the origin (see [32, Figs. 1.1, 1.2]). In the same way that the dynamics of the branch points of the inviscid solution help in understanding the formation of a shock in the real (physical) plane, we intend to illustrate the preservation of regularity of the viscous solution by further analyzing the dynamics of the simple poles. In turn, this will shed some light on the interaction between the nonlinear convective term and the diffusive one present in the (viscous) BE. Furthermore, we clarify the limiting process which describes the vanishing viscosity limit by focusing on the small ν asymptotic behavior of the poles. As $\nu \to 0^+$, the poles condense on the imaginary axis, yielding an asymptotic pole density. The inviscid limit can be recovered by introducing an integral representation of the Mittag–Leffler expansion which involves this density.

These results are presented in [32].

We focus on BE with the same cubic initial data (1.2) used by Bessis and Fournier, whose choice will be clarified. It should be noted, however, that the method of pole dynamics used in this article is adaptable to a large class of one-dimensional evolution equations (cf. [13, 16, 36]). The main difficulty in adapting this method to equations with spatial derivatives of order higher than two is that it may translate into additional algebraic conditions. Thus, one may have to solve a differential-algebraic system of equations (DAE). Additionally, the choice of the initial data need not be fixed and is actually the focus of current research in the case of BE with random initial data. Much attention has recently been devoted to this problem (see, for example, [4, 19, 26, 30, 34]). A final note on the generality of the method: the pole expansion and pole dynamics which are derived for BE are valid for any meromorphic solution to BE and as such correct the pole expansion previously derived for BE.

In part I, we describe exact and asymptotic properties of the positive viscosity solution, its pole locations, and their dynamics.

In section 2, the solution is explicitly given by the Cole–Hopf transform for $\nu > 0$. From a careful analysis of the Cole–Hopf variable, the solution is expressed in terms of its polar singularities by means of a Mittag–Leffler (pole) expansion. A correction to the infinite dimensional CDS derived by Bessis and Fournier which governs the time evolution of the poles is found by replacing the pole expansion of the solution into the PDE. This system represents compatibility conditions for the existence of such a pole expansion.

In section 3, from the integral representation obtained via the Cole–Hopf analysis and by means of the saddle-point method, we derive an asymptotic formula for the solution $u_\nu(x,t)$ for small ν. However, for $t \geq t_*$, there is a degeneracy in the asymptotic formula at the caustic $x = \pm x_s(t)$ where two saddle points coalesce; thus, we derive both the regular saddle-point analysis within and outside the caustic and a uniformly valid expansion via Pearcey's integral, which correctly describes the transition between the two regions. The asymptotic behavior of the solution at the caustic $u_\nu(x_s(t),t)$ is obtained from the Pearcey representation and is shown to match the behavior obtained from the classical saddle-point analysis.

In section 4, we analyze the pole locations: at the inviscid shock time t_* we use the Cole–Hopf variable to approximate the poles. Highly accurate asymptotic formulas of a related Fourier integral derived in [31] enable us to obtain almost exact pole locations independent of the viscosity. At other times ($t \neq t_*$), when no such formula can be obtained, we derive weaker asymptotic results: for small $\nu > 0$ and $0 < t \leq t_*$, we show that the poles are a perturbation of the inviscid branch-point singularities of the form $\beta_k(t,\nu) = |x_s(t)| + \mathcal{O}((k\nu)^{3/4})$. For $t > t_*$, their asymptotic behavior no longer depends on the inviscid branch-point singularities, and it is given by $\beta_k(t,\nu) = \mathcal{O}((k\nu)^{3/4})$. Similarly, we also show that for large k, fixed ν, and all $t > 0$, we have $\beta_k(t,\nu) = \mathcal{O}((k\nu)^{3/4})$.

In section 5, we analyze the time evolution of the poles more explicitly since their actual location for $t \neq t_*$ has not been described. The method consists in numerically solving a truncated version of the CDS. The "initial data" which is adjoined to this truncated system is generated by the exact pole locations found in section 4. A Runge–Kutta–Fehlberg 4–5 time marching scheme is used in combination with the "multipole" algorithm designed by Greengard and Rokhlin [21]. This multipole algorithm reduces the computational complexity of the nonlinear interaction of the poles in the Calogero ODE system from $\mathcal{O}(N^2)$ to $\mathcal{O}(N \log N)$ particles (poles), thereby

allowing us to carry out very large simulations with up to $N = 50,000$ poles. The closed-form solution to a two-pair pole dynamics is obtained and serves as a test case for the multipole simulation. The poles $\pm\beta_k(t,\nu)$ are confined to the imaginary axis and move towards the origin until a time $t = t_u(k)$, $k \in \mathbb{N}^*$; this is the time at which they turn around and move away from the origin. These turn-around times $t_u(k)$ decrease as k increases: $t_u(1) > t_u(2) > \cdots > t_u(n) > \cdots > 0$. Moreover, $t_u(1)$ occurs before t_* for $\nu \gtrapprox .01$ and after t_* for $\nu \lessapprox .01$. Another worthwhile feature is that t_u increases with decreasing ν, in accordance with the fact that the time at which the solution starts decaying increases with decreasing ν.

From this procedure, the evolution of the width of the analyticity strip is shown to remain uniformly bounded away from zero, agreeing with the asymptotic predictions and the well-known fact that BE with analytic initial data has a smooth solution for all times as long as $\nu > 0$ (in agreement with the results of Sulem, Sulem, and Frisch in [35]).

Finally, the solution is computed for small viscosity using pole dynamics, finite differences, and asymptotic methods (saddle-point analysis), and numerical agreement is established. The difference scheme we use is the method of lines consisting of the same Runge–Kutta–Fehlberg 4–5 scheme in time combined with central differencing in space. The solution is reconstructed from the pole positions and the Mittag–Leffler (pole) expansion of the solution.

In part II [32], the zero-viscosity limit of the solution is obtained via a process of pole condensation. It is shown that the asymptotic density of poles, which describes their condensation on the imaginary axis, can be obtained as the weak limit of a discrete Borel measure (analogously to the zero-dispersion limit of the spectral measure in the KdV problem). The analytic structure of the inviscid solution, which is a three-sheeted Riemann surface with three branch-point singularities, is recovered. The continuum limit of the pole expansion of the solution and the CDS for the poles is a system of two integro-differential equations which form a new representation of the solution to the inviscid BE. This formalism clarifies the relation between pole dynamics and branch-cut dynamics. A large wave number asymptotic expansion of the Fourier transform of the inviscid solution uniformly valid in a neighborhood of the shock time is described in terms of the Airy function. This provides a clarification of the degeneracy presented by Fournier and Frisch in [19]. In [33], this methodology is adapted to the dispersive case $\nu \in i\mathbb{R}$.

2. Integral representation, pole expansion, and pole dynamics for $\nu > 0$.

2.1. The Cole–Hopf solution and Mittag–Leffler expansion. The Cole–Hopf solution to the initial value problem (1.1)–(1.2) can be represented by a Mittag–Leffler expansion as follows.

THEOREM 2.1. *For all $\nu, t, t_* > 0$, the solution to BE with initial data $u_0(x) = 4x^3 - x/t_*$ is*

$$u_\nu(x,t) = \frac{x}{t} - 2\nu\,\partial_x \log\big(E_\nu(x,t)\big),$$
$$E_\nu(x,t) = \int_{-\infty}^{\infty} \exp\left\{\frac{1}{2\nu}\left(\frac{x}{t}y + \alpha y^2 - y^4\right)\right\} dy,$$

where $2\alpha = 1/t_* - 1/t \in \mathbb{R}$. For fixed ν, t, $E_\nu(x,t)$ is an even entire function of x of order $4/3$ with countably many simple zeros which come in pure imaginary opposite

and conjugate pairs. Moreover, $E_\nu(x,t)$ has the infinite product representation

$$E_\nu(x,t) = \mathcal{C}_\nu(t)\prod_{n=1}^{\infty}\left(1+\frac{x^2}{\beta_n^2(t,\nu)}\right), \quad \sum_{n=1}^{\infty}\frac{1}{\beta_n}=+\infty, \quad \sum_{n=1}^{\infty}\frac{1}{\beta_n^2}<+\infty,$$
$$\mathcal{C}_\nu(t) = \frac{\sqrt{\alpha}}{2}\,e^{\frac{\alpha^2}{16\nu}}\,K_{1/4}\left(\frac{\alpha^2}{16\nu}\right), \quad \mathcal{C}_\nu(t_*) = \nu^{1/4}2^{-3/4}\Gamma(1/4),$$

where $K_q(z)$ is the modified Bessel function of the second kind. Thus, the solution $u_\nu(x,t)$ has an alternate representation in terms of a Mittag–Leffler (pole) expansion

$$u_\nu(x,t) = \frac{x}{t} - \sum_{n=1}^{\infty}\frac{4\nu x}{x^2+\beta_n^2(t,\nu)} = \frac{x}{t} - 2\nu\sum_{\substack{n=-\infty\\ n\neq 0}}^{\infty}\frac{1}{x-i\beta_n(t,\nu)},$$

which converges uniformly on compact sets for x away from the poles $a_n=\pm i\beta_n$.

Proof. The solution to system (1.1) is constructed using the Cole–Hopf nonlinear transform $u=-2\nu\,\partial_x\log(\phi_\nu)$ [17, 22], which was first introduced by Forsyth (cf. [18, section 207, p. 100]). This nonlinear dependent variable transformation maps BE into the diffusion equation for $\phi_\nu(x,t)$ with corresponding initial data $\phi_0(x)=\exp\{-\frac{1}{2\nu}\int_0^x u_0(y)dy\}$. The solution is therefore represented by means of a convolution:

$$\begin{aligned}\phi_\nu(x,t) &= (K_\nu * \phi_o)(x,t)\\ &= (4\pi\nu t)^{-1/2}\int_{-\infty}^{\infty}\exp\left\{-\frac{(x-y)^2}{4\nu t}-\frac{1}{2\nu}\int_0^y u_0(\eta)d\eta\right\}dy\\ &= K_\nu(x,t)E_\nu(x,t),\end{aligned}$$

where

$$K_\nu(x,t)=K(x,\nu t)=(4\pi\nu t)^{-1/2}\exp\left(-x^2/4\nu t\right)$$

is the fundamental solution of the diffusion equation and

$$E_\nu(x,t)=\int_{-\infty}^{\infty}\exp\left\{\frac{1}{2\nu}\int_0^y\left(\frac{x}{t}-\frac{\eta}{t}-u_0(\eta)\right)d\eta\right\}dy. \tag{2.1a}$$

Since $\partial_x\log\big(K_\nu(x,t)\big)=-x/2\nu t$, the solution of the original problem is given by

$$u_\nu(x,t)=\frac{x}{t}-2\nu\,\partial_x\log\big(E_\nu(x,t)\big). \tag{2.1b}$$

For $u_0(x)=4x^3-x/t_*$, $\nu,t>0$, we obtain the following solution:

$$E_\nu(x,t)=\int_{-\infty}^{\infty}\exp\left\{\frac{1}{2\nu}\left(\frac{x}{t}y+\alpha y^2-y^4\right)\right\}dy, \qquad \alpha=\frac{t-t_*}{2tt_*}\in\mathbb{R}. \tag{2.2}$$

It is clear that E_ν is an even, real analytic function of x and therefore satisfies the conjugacy relation $E_\nu(\overline{x},t)=\overline{E_\nu(x,t)}$ (the analyticity of E_ν can be verified using Morera's theorem). The positive order λ of an entire function $f(z)$ is defined as $\lambda=\limsup_{r\to+\infty}\log\log M(r)/\log r$, where $M(r)=\max_{|z|=r}|f(z)|$. For a fixed time $t>0$, the order of E_ν is the smallest number $\lambda\in\mathbb{R}_+$ such that

$M_\nu(r) = \max_{|x|=r} |E_\nu(x,t)| \le \exp(r^{\lambda+\epsilon})$ for any $\epsilon > 0$ as soon as r is sufficiently large. From the asymptotic behavior of E_ν for $|x| = r \to +\infty$, we find in (4.4) that $M_\nu(r) = \mathcal{O}(r^{1/3}\exp(-\kappa(t)\, r^{4/3}/2\nu))$, where $\kappa(t)/2\nu$ is the "type" of the entire function E_ν. Thus, it is clear that its order is $\lambda = 4/3$. It is known that entire functions of fractional order have infinitely many zeros (see [3, 8]); thus, E_ν has infinitely many zeros that come in opposite and conjugate pairs. Since the fractional order of the entire function E_ν is also the exponent of convergence of its zeros a_n (see again [3, 8]), we have

$$\sum_{n=1}^{\infty} \frac{1}{|a_n|^{\lambda+\epsilon}} < +\infty \ \forall \epsilon > 0. \tag{2.3}$$

Using a Hadamard decomposition, we construct the solution u_ν by factorization of the zeros of E_ν. The canonical infinite product expansion of E_ν is (see [3])

$$E_\nu(x,t) = \mathcal{C} x^m e^{g(x)} \prod_{n=1}^{\infty} \left(1 - \frac{x}{a_n}\right) e^{x/a_n + \frac{1}{2}(x/a_n)^2 + \cdots + \frac{1}{p}(x/a_n)^p},$$

where $g(x)$ is a polynomial of degree q. The integer $h = \max(p,q)$, which is called the genus of the product representation of the entire function E_ν, satisfies the bound $h \le \lambda \le h+1 \Rightarrow h = 1 \Rightarrow p, q \le 1$. Moreover, since E_ν is an even function of x, we must have $q = \deg g(x) = 0$, and therefore $p = 1$ (since $p + 1 > \lambda$, $p \in \mathbb{N}$). Since $\mathcal{C} = \mathcal{C}_\nu(t) = E_\nu(0,t) \neq 0$ (see (2.6a)), we must also set $m = 0$, so the canonical product must be of the form

$$E_\nu(x,t) = \mathcal{C}_\nu(t) \prod_{n=1}^{\infty} \left(1 - \frac{x}{a_n}\right) e^{x/a_n}, \quad \sum_{n=1}^{\infty} \frac{1}{|a_n|} = +\infty, \quad \sum_{n=1}^{\infty} \frac{1}{|a_n|^2} < +\infty.$$

Due to the even parity of E_ν, its zeros come in opposite pairs $x = \pm a_n$; thus, the product representation reduces to the simple form

$$E_\nu(x,t) = \mathcal{C}_\nu(t) \prod_{n=1}^{\infty} \left(1 - \frac{x^2}{a_n^2}\right).$$

In [29], Pólya showed that functions of the form

$$\int_{-\infty}^{\infty} e^{-at^{4n} + bt^{2n} + iyt} dt \qquad n \ge 1,\ a > 0,\ b \in \mathbb{R} \tag{2.4}$$

have only real zeros. Using this property, it is straightforward to show that the zeros of E_ν come in pure imaginary conjugate pairs; thus, we let $a_n = i\beta_n$, $\beta_n > 0$ and obtain an infinite product expansion of E_ν valid for all $t, \nu > 0$:

$$E_\nu(x,t) = \mathcal{C}_\nu(t) \prod_{n=1}^{\infty} \left(1 + \frac{x^2}{\beta_n^2(t,\nu)}\right), \quad \sum_{n=1}^{\infty} \frac{1}{\beta_n} = +\infty, \quad \sum_{n=1}^{\infty} \frac{1}{\beta_n^2} < +\infty, \tag{2.5}$$

where $\mathcal{C}_\nu(t)$ is a constant depending on t which can be found explicitly: let $K_q(z)$ be the modified Bessel function of the second kind; then

$$\mathcal{C}_\nu(t) = E_\nu(0,t) = \int_{-\infty}^{\infty} e^{(\alpha y^2 - y^4)/2\nu}\, dy = \frac{\sqrt{\alpha}}{2}\, e^{\frac{\alpha^2}{16\nu}}\, K_{1/4}\left(\frac{\alpha^2}{16\nu}\right), \tag{2.6a}$$

$$\mathcal{C}_\nu(t_*) = E_\nu(0,t_*) = \int_{-\infty}^{\infty} e^{-y^4/2\nu}\, dy = \nu^{1/4} 2^{-3/4} \Gamma(1/4), \tag{2.6b}$$

with $K_{1/4}(z) = \mathcal{O}(z^{-1/4})$ as $z \to 0$. After logarithmic differentiation of E_ν and by using (2.1b) and (2.5), the spatially singular part of the solution being the ratio of two entire functions is meromorphic. Thus, we obtain a Mittag–Leffler expansion of the solution which we refer to as the pole expansion:

$$u_\nu(x,t) = \frac{x}{t} - \sum_{n=1}^{\infty} \frac{4\nu x}{x^2 + \beta_n^2(t,\nu)} = \frac{x}{t} - 2\nu \sum_{\substack{n=-\infty \\ n\neq 0}}^{\infty} \frac{1}{x - i\beta_n(t,\nu)}. \tag{2.7}$$

In the second sum, we have adopted the convention that $\beta_{-n} = -\beta_n$. Furthermore, it must be understood as a symmetric (convergent) sum of the form

$$\sum_{\substack{n=-\infty \\ n\neq 0}}^{\infty} \frac{1}{x - i\beta_n(t,\nu)} = \sum_{n\in\mathbb{N}^*} \left(\frac{1}{x - i\beta_n(t,\nu)} + \frac{1}{x + i\beta_n(t,\nu)} \right).$$

Since $\sum_n \beta_n^{-2} < \infty$ for any fixed $t, \nu > 0$, the series defining u_ν in (2.7) converges absolutely and uniformly on any strip $0 < \beta_k < \delta_k \leq |\Im x| \leq \delta_{k+1} < \beta_{k+1}$, $k \in \mathbb{N}^* = \mathbb{N}\backslash\{0\}$. Therefore, u_ν is analytic in the strip $|\Im x| < \beta_1$ where $i\beta_1$ is the first ordered pole on the imaginary axis. From (2.7), u_ν conserves the odd parity of the initial data as expected from the PDE: $u_\nu(-x,t) = -u_\nu(x,t)$. In order for this pole expansion to make sense, the behavior of the spatially singular part of the expansion should be unbounded as $t \to 0^+$ in order to balance with the term x/t. □

2.2. CDS for the poles $\boldsymbol{\beta_n(t,\nu)}$. We describe the time evolution of the poles $\beta_n(t,\nu)$ according to an infinite dimensional dynamical system which is found as a compatibility condition for the existence of the pole expansion (2.7). We prove the following property.

PROPERTY 2.2. *The imaginary part $\beta_n = \beta_n(t,\nu) : \mathbb{R}_+ \times \mathbb{R}_+ \to \mathbb{R}_+$ of the simple poles $x = \pm i\beta_n$ of $u_\nu(x,t)$ satisfy the Calogero-type infinite-dimensional dynamical system*

$$\dot\beta_n = \frac{\beta_n}{t} + \frac{\nu}{\beta_n} - 4\nu\beta_n \sum_{\substack{l=1 \\ l\neq n}}^{\infty} \frac{1}{\beta_l^2 - \beta_n^2} \ \forall n \in \mathbb{N}^*.$$

Adopting the convention that $\beta_{-n} = -\beta_n$, we have a symmetric formulation:

$$\dot\beta_n = \frac{\beta_n}{t} - 2\nu \sum_{\substack{l=-\infty \\ l\neq n,0}}^{\infty} \frac{1}{\beta_l - \beta_n} \ \forall n \in \mathbb{Z}^*.$$

Moreover, the variables $\gamma_n(t,\nu) = \beta_n^2(t,\nu)/\nu$ satisfying $\sum_n \gamma_n^{-1} < +\infty$ are the solution to the ν-independent infinite system of ODEs:

$$\frac{\dot\gamma_n}{2} = \frac{\gamma_n}{t} + 1 - 4\gamma_n \sum_{\substack{l=1 \\ l\neq n}}^{\infty} \frac{1}{\gamma_l - \gamma_n} \ \forall n \in \mathbb{N}^*.$$

Proof. The usual pole expansion that is sought in [1, pp. 203–209] and [13, 16, 20] is of the form

$$u_\nu = \sum_{n=1}^{N} \frac{2\nu}{x - i\beta_n}. \tag{2.8}$$

However, as $N \to +\infty$ this series diverges for any fixed x, t, ν. Since we know that the representation (2.7) converges away from the poles (since $\sum_n \beta_n^{-2} < \infty$ from (2.5)) instead of using (2.8), we replace the full Mittag–Leffler/pole expansion (2.7) in the PDE (1.1). The extension from a finite pole expansion to an infinite one is easily made (cf. [16, section 3]). We obtain an infinite system of ODEs which govern the motion of the poles $\beta_n(t,\nu)$ as they evolve with time for $t > 0$. We introduce the following notations:

$$\dot{\beta}_n = \frac{d\beta_n}{dt}, \qquad \sum_n = \sum_{n=1}^{\infty}, \qquad \sum_l = \sum_{l=1}^{\infty}, \qquad \sum_{l\neq n} = \sum_{\substack{l=1 \\ l\neq n}}^{\infty}.$$

Using partial fraction expansion we have the following property.

PROPERTY 2.3. *Let $x \notin \{i\beta_n \in i\mathbb{R}$ for all $n \in \mathbb{Z}^*\}$ and $l \neq n$; then*

$$\frac{1}{(x^2+\beta_n^2)(x^2+\beta_l^2)} = \frac{1}{\beta_n^2-\beta_l^2}\cdot\left(\frac{1}{x^2+\beta_l^2} - \frac{1}{x^2+\beta_n^2}\right) \tag{2.9a}$$

$$\frac{1}{(x^2+\beta_n^2)(x^2+\beta_l^2)^2} = \frac{1}{(\beta_l^2-\beta_n^2)^2}\cdot\left(\frac{1}{x^2+\beta_n^2} - \frac{1}{x^2+\beta_l^2}\right) + \frac{1}{\beta_n^2-\beta_l^2}\cdot\frac{1}{(x^2+\beta_l^2)^2}. \tag{2.9b}$$

Due to obvious symmetries, we also have

$$\sum_n \sum_{l\neq n} \frac{1}{(\beta_n^2-\beta_l^2)^2}\cdot\left(\frac{1}{x^2+\beta_n^2} - \frac{1}{x^2+\beta_l^2}\right) = 0. \tag{2.10}$$

Thus, combining (2.9b) and (2.10), we obtain Property 2.4.

PROPERTY 2.4. *Let $x \notin \{i\beta_n \in i\mathbb{R}$ for all $n \in \mathbb{Z}^*\}$; then*

$$\begin{aligned}\sum_n \sum_{l\neq n} \frac{1}{(x^2+\beta_n^2)}\cdot\frac{1}{(x^2+\beta_l^2)^2} &= \sum_n \sum_{l\neq n} \frac{1}{\beta_n^2-\beta_l^2}\cdot\frac{1}{(x^2+\beta_l^2)^2} \\ &= \sum_n \sum_{l\neq n} \frac{1}{\beta_l^2-\beta_n^2}\cdot\frac{1}{(x^2+\beta_n^2)^2}.\end{aligned}$$

After replacing the pole expansion (2.7) into the original PDE (1.1), canceling the terms $\pm x/t^2$, regrouping terms together in powers of $(x^2+\beta_n^2)^{-1}$, dividing by $8\nu x$, and appealing to both equation (2.9a) of Properties 2.3 and 2.4, Property 2.2 is proved. Note that in [7], the pole interaction in the dynamical system was incorrectly stated as a divergent semi-infinite sum of the form

$$\dot{\beta}_n = \frac{\beta_n}{t} - 2\nu \sum_{\substack{l\geq 1 \\ l\neq n}} \frac{1}{\beta_l - \beta_n}.$$

Due to the generality of the integral representation (2.1a,b) of solutions to an initial value problem (IVP) for BE, it is important to see that the pole representation

(2.7) and pole dynamics of Property 2.2 are special cases of the general representation for a meromorphic solution to BE.

PROPERTY 2.5. *Let $\mathcal{I} \subseteq \mathbb{Z}$ be a set of indices, either finite or countable, and let $\{a_n(t,\nu), n \in \mathcal{I}\}$ be a finite or countable set of time-dependent pole locations. Then any meromorphic solution with poles $\{a_n(t,\nu), n \in \mathcal{I}\}$ must have the following pole representation/pole dynamics:*

$$\textit{Pole representation:} \quad u_\nu(x,t) = \frac{x}{t} - 2\nu \sum_{n\in\mathcal{I}} \frac{1}{x - a_n(t,\nu)},$$

$$\textit{Pole dynamics:} \quad \dot{a}_n = \frac{a_n}{t} - 2\nu \sum_{\substack{l\in\mathcal{I} \\ l\neq n}} \frac{1}{a_n - a_l} \qquad \forall n \in \mathcal{I}.$$

Moreover, if the initial data is odd, then the poles must come in opposite pairs $\{a_{\pm n}(t,\nu), n \in \mathcal{I} \subseteq \mathbb{Z}^* = \mathbb{Z}\backslash\{0\} \mid \ a_{-n} = -a_n\}$. In this case, the pole representation is fully symmetric.

3. Asymptotic analysis of $u_\nu(x,t)$ as $\nu \to 0^+$, $t > t_*$. When $\nu \to 0^+$, we evaluate the asymptotic behavior of E_ν using the saddle-point method. The caustic $x = x_s(t)$ corresponds to the envelope of the characteristics of the inviscid Burgers solution and is also determined by the following system of equations:

$$\begin{cases} 0 = w_z(z,x) = x/t + 2\alpha z - 4z^3, \\ 0 = w_{zz}(z,x) = 2\alpha - 12z^2, \end{cases} \tag{3.1}$$

where

$$w(z,x) = \int_0^z \left(\frac{x}{t} - \frac{\eta}{t} - u_0(\eta)\right) d\eta \tag{3.2}$$

is the phase function of the integrand in the definition of $E_\nu(x,t)$. This system represents the conditions for the phase function w to have saddle points of multiplicity two, thereby yielding a curve in the (x,t) plane on which two saddle points of multiplicity one coalesce into a saddle point of multiplicity two. From the second equation in (3.1), we find $z_{caustic}(t) = \pm\sqrt{\alpha/6}$; from the first, we have

$$x = x_{caustic} = t\big(4z_{caustic}(t)^3 - 2\alpha z_{caustic}(t)\big) = \mp t\left(\frac{2\alpha}{3}\right)^{3/2} = \mp x_s(t), \tag{3.3}$$

where $x_s(t) = (3t_*)^{-3/2}(t-t_*)^{3/2}t^{-1/2}$ is the second-order branch point of the inviscid solution described in [32, App. C]. We find that all three saddle points may be relevant within the caustic $|x| < |x_s(t)| - \delta/2$, where $\delta > 0$. For a discussion on such caustics, cf. [24, 28]. When $t > t_*$, $x \in \big(-\infty, -x_s(t) - \delta/2\big) \cup \big(x_s(t) + \delta/2, \infty\big)$, $\nu \to 0^+$, the same analysis holds and one recovers the characteristic solution outside the caustic consisting of only one relevant saddle point. The transition from within the caustic to outside is not uniform as the asymptotic behavior at the caustic $x = \pm x_s(t)$ is degenerate (two saddle points have coalesced). The transitionary regime from one relevant saddle point to two at and around the caustic is therefore described by means of the Pearcey integral which allows for a uniformly valid description.

3.1. Inner expansion: $x \in \big(-x_s(t)+\delta/2,\ x_s(t)-\delta/2\big)$, $\delta > 0$, $t > t_*$. In the analysis that follows, we are only concerned with the dominant behavior of E_ν; thus, we only retain the first term:

$$E_\nu(x,t) = \sum_{s=0,1,2} \sqrt{\frac{-4\pi\nu}{w_{zz}(z_s,x)}}\exp\left(\frac{w\big(z_s,x\big)}{2\nu}\right)\Big(1+\mathcal{O}(\nu)\Big), \tag{3.4}$$

as $\nu \to 0^+$, with

$$w_z\big(z_s(x,t),x\big) = 0, \quad w_{zz}\big(z_s(x,t),x\big) = 2\alpha - 12z_s^2. \tag{3.5}$$

Since

$$0 = \frac{z_s}{4}w_z\big(z_s,x\big) = \frac{xz_s}{4t} + \frac{\alpha}{2}z_s^2 - z_s^4,$$

we have that

$$w\big(z_s(x,t),x\big) = \frac{x}{t}z_s + \alpha z_s^2 - z_s^4 = \frac{3}{4}\frac{x}{t}z_s + \frac{\alpha}{2}z_s^2. \tag{3.6}$$

The values of the saddle points $z_s = z_s(x,t)$ of (3.4) are determined by the three roots of the first equation in system (3.1), i.e., the first equation of (3.5). They are, specifically,

$$\begin{cases} z_0 = \omega\,\mathcal{A} + \omega^2\,\mathcal{B}, \\ z_1 = \omega^2\,\mathcal{A} + \omega\,\mathcal{B}, \\ z_2 = \mathcal{A} + \mathcal{B}, \end{cases} \tag{3.7}$$

where $w = e^{2\pi i/3}$ is a cube root of unity and

$$\begin{cases} \mathcal{A}(x,t) = (8t)^{-1/3}\cdot\sqrt[3]{x+\sqrt{x^2-x_s^2}}, \\ \mathcal{B}(x,t) = (8t)^{-1/3}\cdot\sqrt[3]{x-\sqrt{x^2-x_s^2}}. \end{cases} \tag{3.8}$$

Note that all three saddle points are real when $x, x_s \in \mathbb{R}$ and the discriminant $\Delta = x^2 - x_s^2 < 0$, that is, $|x| < |x_s(t)|$. In this case, $\mathcal{A} = \overline{\mathcal{B}}$ (see [32, App. B]). Therefore, we have $z_s \in \mathbb{R}$, $w(z_s,x) \in \mathbb{R}$, and $w_{zz}(z_s,x) = 2\alpha - 12z_s^2 \in \mathbb{R}$. Hence, all three terms in the summation signs may be relevant. Note, however, that the expansion derived for E_ν is only valid within $|x| < |x_s|$, and in order to get an expansion uniformly valid across $x = \pm x_s$ one needs to derive a uniform expansion as presented in section 3.3. The dominant behavior of the solution $u_\nu(x,t)$ is found from the Cole–Hopf representation, so within the caustic $|x| < |x_s| - \delta/2$ we have

$$\begin{aligned} \frac{U_\nu(x,t)}{t} &= 2\nu\,\partial_x\log\big(E_\nu(x,t)\big) \\ &= 2\nu\,\partial_x\log\left(\sum_{s=0,1,2}\sqrt{\frac{-4\pi\nu}{w_{zz}(z_s,x)}}e^{\frac{w(z_s,x)}{2\nu}}\big(1+\mathcal{O}(\nu)\big)\right) \\ &= 2\nu\,\frac{\sum_{s=0,1,2}\partial_x\left(\sqrt{\frac{-4\pi\nu}{w_{zz}(z_s,x)}}e^{\frac{w(z_s,x)}{2\nu}}\right)}{\sum_{s=0,1,2}\sqrt{\frac{-4\pi\nu}{w_{zz}(z_s,x)}}e^{\frac{w(z_s,x)}{2\nu}}} + \mathcal{O}(\nu^2). \end{aligned}$$

Since $w(z_s,x)\in\mathbb{R}$, $\nu>0$, and

$$\frac{\partial w}{\partial x}(z_s,x)=\frac{z_s}{t}, \tag{3.9}$$

we find

$$U_\nu(x,t)=\frac{\sum_{s=0,1,2} z_s\cdot e^{\frac{w(z_s,x)}{2\nu}}/\sqrt{w_{zz}(z_s,x)}}{\sum_{s=0,1,2} e^{\frac{w(z_s,x)}{2\nu}}/\sqrt{w_{zz}(z_s,x)}}+\mathcal{O}(\nu). \tag{3.10}$$

The x-differentiation of the asymptotic formula of $E_\nu(x,t)$ is justified due to the analytic dependency in x. Often one of the three saddle points is such that $w(z_s,x)<0$, and as such, its contribution is exponentially smaller than either of the other two. In terms of the numerical computation that will be carried out in section 5, leaving this term in (3.1) does not affect the value of u_ν. Thus, we can simplify expression (3.10) to a two-term asymptotic expansion that is similar to the one in [38, section 4.2]. Clearly, the further away we are from the caustic, the more dominant one of the saddle points becomes. However, since there is a point where the dominance of one over the other changes (i.e., where they are equally relevant), we must leave both in the asymptotic formula. Note also that $w_{zz}(z_s,x)\to\infty$ as $x\to x_s$, which is characteristic of the degeneracy of the asymptotic formula (3.10) at the caustic $x=x_s$.

PROPERTY 3.1. *For $x\in\big(-x_s(t)+\delta/2,x_s(t)-\delta/2\big)$, $\delta>0$, $t>t_*$, the inner expansion of the solution to BE as $\nu\to0^+$ is given by*

$$u_\nu(x,t)=\frac{x}{t}-\frac{U_\nu(x,t)}{t},$$
$$U_\nu(x,t)=\frac{\sum_{\{s:w(z_s,x)>0\}} z_s\cdot e^{\frac{w(z_s,x)}{2\nu}}/\sqrt{w_{zz}(z_s,x)}}{\sum_{\{s:w(z_s,x)>0\}} e^{\frac{w(z_s,x)}{2\nu}}/\sqrt{w_{zz}(z_s,x)}}+\mathcal{O}(\nu).$$

3.2. Outer expansion: $x\in\big(-x_s(t)-\delta/2,x_s(t)+\delta/2\big)^c$, $\delta>0$, $t>t_*$. The inviscid limit is found in a straightforward manner in this case: only one saddle point is relevant, so the asymptotic limit derived in section 3.1 reduces to

$$U_\nu(x,t)=U(x,t)+\mathcal{O}(\nu)\qquad\text{as }\nu\to0^+,$$

where $U(x,t)=z_{s*}(x,t)$ is the spatially singular part of the inviscid solution (see [32, App. C]). The particular saddle point z_{s*} that is chosen at every x is the one for which $w(z_{s*},x)=\max_{s=0,1,2} w(z_s,x)$. Hence, we have the following property outside of the caustic.

PROPERTY 3.2. *Let $\delta>0$, $t>t_*$, and define $z_{s*}(x,t)$ by*

$$w(z_{s*},x)=\max_{s=0,1,2} w(z_s,x).$$

Then for $x\in\big(-x_s(t)-\delta/2,x_s(t)+\delta/2\big)^c$, the solution to BE is given by

$$u_\nu(x,t)=\frac{x}{t}-\frac{U_\nu(x,t)}{t}=\frac{x}{t}-\frac{U(x,t)}{t}+\mathcal{O}(\nu)\qquad\text{as }\nu\to0^+,$$

where $U(x,t)=z_{s*}(x,t)$ is the Lagrangian characteristic variable of the inviscid solution.

3.3. Uniform asymptotic expansion as $\nu \to 0^+$ in a neighborhood of the caustics $x = \pm x_s(t)$ for $t > t_*$ via Pearcey's integral. Following the notation of Kaminski in [24], we introduce the Pearcey integral from which one can derive a uniform asymptotic expansion with two coalescing saddle points (see [15]): let

$$P(X,Y) = \int_{-\infty}^{+\infty} e^{i\left(v^4/4 + Xv^2/2 + Yv\right)}\, dv \tag{3.11}$$

denote the Pearcey integral. Introducing the change of variable

$$y \to (-i\nu/2)^{1/4}\, v = (\nu/2)^{1/4}\, e^{3\pi i/8}\, v$$

and deforming the path of integration back to the real axis using Jordan's lemma, we can express $E_\nu(x,t)$ as

$$\begin{aligned} E_\nu(x,t) &= \int_{-\infty}^{+\infty} \exp\left\{\frac{1}{2\nu}\left(\frac{x}{t}y + \alpha y^2 - y^4\right)\right\} dy \\ &= \left(\frac{-i\nu}{2}\right)^{1/4} \int_{-\infty}^{+\infty} \exp\left\{ i\left(\frac{v^4}{4} + \frac{\alpha e^{i\pi/4}}{\sqrt{2\nu}}\frac{v^2}{2} + \frac{x e^{-i\pi/8}}{2t}\left(\frac{1}{2\nu^3}\right)^{1/4} v\right)\right\} dv \\ &= \left(\frac{-i\nu}{2}\right)^{1/4} P\left(X = \frac{\alpha e^{i\pi/4}}{\sqrt{2\nu}}, Y = \frac{x e^{-i\pi/8}}{2t}\left(\frac{1}{2\nu^3}\right)^{1/4}\right). \end{aligned} \tag{3.12}$$

Clearly, a small ν asymptotic of E_ν is equivalent to a combined asymptotic expansion of the Pearcey integral as $|X|, |Y| \to +\infty$. The caustic of $P(X,Y)$ and the corresponding caustic of $E_\nu(x,t)$ is given by

$$Y = \frac{2}{\sqrt{27}}(-X)^{3/2} \Longleftrightarrow x = \pm x_s(t) \in \mathbb{R} \quad \text{for } t > t_*. \tag{3.13}$$

Hence, the uniform asymptotic behavior of E_ν in a neighborhood of the caustic is found from the one of $P(-X, (2/\sqrt{27} - \tau)X^{3/2})$ as $X \to +\infty$, where $\tau = 0$ at the caustic and $\tau \neq 0$ away from it (see [24]). This amounts to a uniformly valid expansion in the interval $|x \pm x_s(t)| \leq |\delta_\pm(\tau;t)|$, where $\delta_\pm(\tau) = \delta_\pm(\tau;t) = \mp\sqrt{27}x_s(t)\cdot\tau/2 \in \mathbb{R}$. This expansion is also valid outside of this interval, however the region of interest is a neighborhood of the caustic. Indeed one only needs to use the asymptotic expansion of the Airy function and its derivative to find the results obtained in sections 3.1 and 3.2. From (3.12) we have that

$$\begin{aligned} U_\nu(x,t) &= t\cdot 2\nu\,\partial_x \log\big(E_\nu(x,t)\big) \\ &= t\cdot 2\nu\,\partial_x \log\left[P\left(X(\nu;t) = \frac{\alpha e^{i\pi/4}}{\sqrt{2\nu}}, Y(\nu;x,t) = \frac{x e^{-i\pi/8}}{2t}\left(\frac{1}{2\nu^3}\right)^{1/4}\right)\right]. \end{aligned}$$

Let

$$X = X(\nu;t), \qquad Y = Y(\nu;x,t) = Y(\nu; x = \pm x_s(t) - \delta_\pm(\tau;t), t),$$

where $\delta_\pm(\tau;t) \to 0^\mp$ as $\tau \to 0^\pm$, so that

$$\begin{aligned} U_\nu\Big(x = \pm x_s(t) - \delta_\pm(\tau;t), t\Big) &= t\cdot 2\nu\,\partial_x \log P(X,Y) \\ &= -t\cdot 2\nu\,\partial_\tau \log\Big(P\left(-X, (2/\sqrt{27} - \tau)X^{3/2}\right)\Big) \Big/ \frac{\partial \delta_\pm}{\partial \tau}\,. \end{aligned}$$

Let $P(\tau) = P\left(-X, (2/\sqrt{27} - \tau)X^{3/2}\right)$. Then, since $\partial\delta_\pm/\partial\tau = \mp\sqrt{27}x_s(t)/2$, we have

$$U_\nu\Big(x = \pm x_s(t) - \delta_\pm(\tau;t), t\Big) = \pm\frac{4\nu t}{\sqrt{27}x_s(t)}\frac{P_\tau(\tau)}{P(\tau)}.$$

Let

$$Ai(z) = \frac{1}{2\pi i}\int_{-i\infty}^{i\infty} e^{v^3/3 - zv}\,dv$$

stand for the Airy function (cf. [2]); then the following property is found in [24].

PROPERTY 3.3. *The uniform asymptotic expansion of* $P(-X, (\frac{2}{\sqrt{27}} - \tau)X^{3/2})$ *as* $X \to +\infty$ *in a neighborhood of* $\tau = 0$ *is given by*

$$P\left(-X, \left(\frac{2}{\sqrt{27}} - \tau\right)X^{3/2}\right) = \left[e^{iX^2[f(v_2)+f(v_3)]/2}\left\{p_0(\tau)\frac{2\pi}{X^{1/6}}Ai(-X^{4/3}\zeta(\tau))\right.\right.$$
$$\left.\left. + q_0(\tau)\frac{2\pi}{iX^{5/6}}Ai'(-X^{4/3}\zeta(\tau))\right\} + e^{iX^2 f(v_1)}\left(\frac{\pi}{3v_1^2 - 1}\right)^{1/2}\frac{1+i}{X^{1/2}}\right]\left(1 + \mathcal{O}\left(\frac{1}{X^2}\right)\right),$$

with

$$p_0(\tau) = 3^{-1/6}(1 + \mathcal{O}(\tau)), \quad q_0(\tau) = -\frac{3^{-5/6}}{2}(1 + \mathcal{O}(\tau)), \quad \zeta(\tau) = 3^{-1/6}\tau(1 + \mathcal{O}(\tau)),$$

and

$$f(v) = f(v;\tau) = \frac{v^4}{4} - \frac{v^2}{2} + \left(\frac{2}{\sqrt{27}} - \tau\right)v,$$

and the $v_i, i = 1,2,3$ *are the saddle points of* $f(v;\tau)$ *determined by the equation* $f_v(v_i;\tau) = 0$, *so* $f(v_i;\tau) = -v_i^2/4 + (2/\sqrt{27} - \tau)3v_i/4$. *The* v_i*'s are, specifically,*

$$v_1(\tau) = -\frac{2}{\sqrt{3}}\sin\left(\frac{\pi}{3} + \phi(\tau)\right), v_2(\tau) = \frac{2}{\sqrt{3}}\sin(\phi(\tau)), v_3(\tau) = \frac{2}{\sqrt{3}}\sin\left(\frac{\pi}{3} - \phi(\tau)\right),$$

where

$$\phi = \phi(\tau) = \frac{1}{3}\arcsin\left(1 - \tau\sqrt{27}/2\right), \quad \tau \in \mathbb{R}, \quad |\phi| \le \frac{\pi}{6}.$$

In order to derive the uniform asymptotic expansion of the derivative P_τ, one can differentiate termwise the expression in Property 3.3 due to the analytic dependency of $P(X,Y)$ in both its arguments X, Y (see [24] and [37, p. 52]). Therefore, since

$$X = \frac{\alpha e^{i\pi/4}}{\sqrt{2\nu}} \Rightarrow \frac{iX^2}{2} = -\frac{\alpha^2}{4\nu} \Rightarrow X^{-2} = \mathcal{O}(\nu)$$

and

$$\frac{\partial f}{\partial\tau}(v_i;\tau) = -v_i, \quad \frac{\partial f}{\partial v}(v_i;\tau) = 0 \quad \Rightarrow \quad \frac{df}{d\tau}(v_i(\tau);\tau) = -v_i(\tau),$$

and using the fact that $2\alpha/3 = (x_s/t)^{2/3}$, the next property is proved.

PROPERTY 3.4. *Let* $\delta_\pm(\tau;t) = \mp\sqrt{27}x_s(t)\cdot\tau/2$. *Then the uniform asymptotic expansion as* $\nu\to 0^+$ *of* $U_\nu(x=\pm x_s(t)-\delta_\pm(\tau;t),t)$ *in a neighborhood of the caustic* $x=\pm x_s(t)$ *is*

$$U_\nu\Big(x=\pm x_s(t)-\delta_\pm(\tau;t),t\Big) = \pm\frac{\sqrt{3}}{2}\left(\frac{x_s(t)}{t}\right)^{1/3}\times\Bigg[[v_2+v_3]e^{-\frac{\alpha^2}{4\nu}[f(v_2)+f(v_3)]}$$
$$\times\left\{p_0(\tau)\frac{2\pi}{X^{1/6}}Ai(-X^{4/3}\zeta(\tau))+q_0(\tau)\frac{2\pi}{iX^{5/6}}Ai'(-X^{4/3}\zeta(\tau))\right\}$$
$$+2v_1\,e^{-\frac{\alpha^2}{4\nu}2f(v_1)}\left(\frac{\pi}{3v_1^2-1}\right)^{1/2}\frac{1+i}{X^{1/2}}\Bigg]$$
$$\Bigg/\Bigg[e^{-\frac{\alpha^2}{4\nu}[f(v_2)+f(v_3)]}\left\{p_0(\tau)\frac{2\pi}{X^{1/6}}Ai(-X^{4/3}\zeta(\tau))+q_0(\tau)\frac{2\pi}{iX^{5/6}}Ai'(-X^{4/3}\zeta(\tau))\right\}$$
$$+e^{-\frac{\alpha^2}{4\nu}2f(v_1)}\left(\frac{\pi}{3v_1^2-1}\right)^{1/2}\frac{1+i}{X^{1/2}}\Bigg]+\mathcal{O}(\nu)\qquad \text{as } \nu\to 0^+.$$

3.3.1. Behavior at the caustics $x=\pm x_s(t)$. At the caustics $x=\pm x_s(t)$, $\tau=0$, $\phi(0)=\pi/6$, $v_1(0)=-2/\sqrt{3}$, and $v_2(0)=v_3(0)=1/\sqrt{3}$. Moreover, $f(v_i;0)=-v_i^2/4+v_i/2\sqrt{3}$, so $f(v_2;0)=f(v_3;0)=-2/3$ and $f(v_1;0)=1/12$. Since $f(v_2;0)<0$ and $f(v_1;0)>0$, the dominant term as $\nu\to 0^+$ in both the numerator and denominator of U_ν is obviously the one containing the exponentially increasing factor $\exp(-\frac{\alpha^2}{4\nu}[f(v_2)+f(v_3)])$. Therefore, the dominant behavior of $U_\nu(\pm x_s(t),t)$ reduces to the simple form

$$U_\nu(\pm x_s(t),t) = \pm\frac{\sqrt{3}}{2}\left(\frac{x_s(t)}{t}\right)^{1/3}\cdot(v_2(0)+v_3(0))+\mathcal{O}(\nu)$$
$$= \pm\left(\frac{x_s(t)}{t}\right)^{1/3}+\mathcal{O}(\nu)\quad \text{as } \nu\to 0^+.$$

Thus, since $u_\nu(x,t)=x/t-U_\nu(x,t)/t$ and from the odd parity of u_ν, we have the following property.

PROPERTY 3.5. *The asymptotic behavior of the solution* $u_\nu(x,t)$ *as* $\nu\to 0^+$ *at the caustic* $x=\pm x_s(t)$ *for* $t>t_*$ *is*

$$u_\nu(\pm x_s(t),t) = \pm\frac{x_s(t)}{t}\mp\frac{1}{t}\left(\frac{x_s(t)}{t}\right)^{1/3}+\mathcal{O}(\nu).$$

This matches the solution found from a classical saddle-point analysis obtained by combining (3.2) and (3.7): when $x=x_s(t)$, both saddle points z_0, z_1 coalesce into $z_s=(x_s(t)/t)^{1/3}$. From the asymptotic formula

$$u_\nu(x,t)=\frac{x}{t}-\frac{z_s(x,t)}{t}+\mathcal{O}(\nu)$$

derived in section 3.2, Property 3.5 is verified. Note that this expression is valid only for $t\geq t_*+\varepsilon$, $\varepsilon>0$.

4. Pole locations.

4.1. Exact pole location at $t = t_*$. From the integral representation (2.2), a Taylor expansion about $x = 0$ can be obtained when $t = t_*$.

PROPERTY 4.1. *Let*

$$\mathcal{S}_\nu(z) = \nu^{1/4}\, 2^{-3/4} \sum_{n=0}^{\infty} (-1)^n \frac{\Gamma(\frac{2n+1}{4})}{\Gamma(2n+1)}\, z^{2n}, \qquad |z| < +\infty,$$

which converges absolutely and uniformly on compact sets for z. Then

$$E_\nu(x, t_*) = \mathcal{S}_\nu\left(\frac{ix}{4t_*}(2\nu)^{-3/4}\right), \qquad |x| < +\infty.$$

Let $x = i\beta$, $\beta \in \mathbb{R}$, $|\beta| < +\infty$; then if we introduce the scaling

$$\beta = \beta(t_*, \nu) = 4t_*(2\nu\mu)^{3/4}, \tag{4.1}$$

we have

$$E_\nu\left(i \cdot 4t_*(2\nu\mu)^{3/4}, t_*\right) = \mathcal{S}_\nu\left(\mu^{3/4}\right). \tag{4.2}$$

Following this scaling, we transform the integral representation of $E_\nu(i\beta, t_*)$ to simplify its analysis. At the inviscid shock time t_*,

$$E_\nu(i\beta, t_*) = \int_{-\infty}^{\infty} \exp\left\{\frac{1}{2\nu}\left(\frac{i\beta}{t_*}y - y^4\right)\right\} dy,$$

and the change of variable

$$y \to \left(\frac{\beta}{4t_*}\right)^{1/3} z \tag{4.3}$$

introduces the scaling factor (4.1) between the imaginary part β_n of the zeros a_n and the viscosity ν. This allows us to express $E_\nu(i\beta, t_*)$ in terms of a new function $F(\mu)$, which has the advantage that its saddle points are fixed to the unit disc (thereby making the asymptotic analysis simpler):

$$E_\nu(i\beta, t_*) = \left(\frac{\beta}{4t_*}\right)^{1/3} F\left(\frac{1}{2\nu}\left(\frac{\beta}{4t_*}\right)^{4/3}\right), \quad F(\mu) = \int_{-\infty}^{\infty} e^{\mu(4iz - z^4)} dz. \tag{4.4}$$

Once the zeros $\{\mu_k\}_{k=1}^{\infty}$ of $F(\mu)$ are found (independent of ν), the poles $\pm a_k(t_*, \nu) = \pm i\beta_k(t_*, \nu)$ of $u_\nu(x, t_*)$ are given by the relation

$$\beta_k(t_*, \nu) = 4t_*(2\nu\mu_k)^{3/4} \quad \forall \nu > 0, \tag{4.5}$$

which was introduced in (4.1). It is important to see that this relation is valid regardless of whether ν is small or β is large. Thus, if we can describe the μ_k's accurately, then the pole locations are known with great precision at t_* (independent of ν). Furthermore, the expansion of $E_\nu(i\beta, t_*)$ as $\nu \to 0^+$ or as $\beta \to +\infty$ is determined by that of $F(\mu)$ as $\mu \to +\infty$. The following theorem is proved in [31].

THEOREM 4.2. *The asymptotic expansion of $F(\mu) = \int_{-\infty}^{\infty} e^{\mu(4iz - z^4)} dz$ as $\mu \to +\infty$ centered about the sector $|\arg \mu| < \pi/2$ is*

$$F(\mu) = \sqrt{\frac{2\pi}{3\mu}} e^{-\frac{3}{2}\mu} \left[\cos\left(3\frac{\sqrt{3}}{2}\mu - \frac{\pi}{6}\right) + \mathcal{O}\left(\frac{1}{\mu}\right)\right] \quad \text{as } \mu \to +\infty.$$

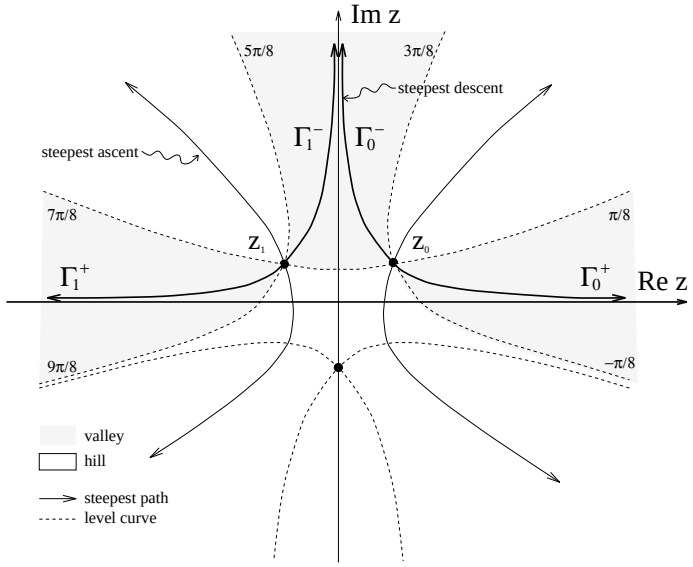

FIG. 4.1. *Hills, valleys, level curves, and steepest paths of the saddle points* $z_0 = e^{i\pi/6}$, $z_1 = e^{i5\pi/6}$ *relevant to the expansion of* $F(\mu) = \int_{-\infty}^{\infty} e^{\mu(4iz - z^4)} dz$ *as* $\mu \to +\infty$.

Moreover, the k*th ordered positive zero* μ_k *of* $F(\mu)$ *for* $k \geq 1$ *is given by*

$$\mu_k^{(0)} = \frac{2\pi}{3\sqrt{3}}(k - 1/3), \qquad \mu_k = \mathcal{G}\left(\mu_k^{(0)}\right) + \mathcal{O}\left(\frac{1}{k^6}\right) \quad \text{as } k \to +\infty,$$
$$\mathcal{G}(\mu) = \mu + \frac{7}{432\mu}\left(1 - \frac{1}{6\mu}\left(1 + \frac{7}{72\mu}\left(1 - \frac{5}{12\mu}\left(1 + \frac{53143}{18900\mu}\right)\right)\right)\right).$$

In addition to this asymptotic description, the first nine values of μ_k are computed numerically in [31] and are listed in section 5. The accuracy of this asymptotic approximation is discussed in [31]; the necessity for such high accuracy will be apparent in section 5. Combining (4.5) and Theorem 4.2, the pole locations at $t = t_*$ are given by the simple form in Property 4.3.

PROPERTY 4.3. *For all* $\nu > 0$,

$$\beta_k(t_*, \nu) = 4t_* \left(\frac{4\nu\pi}{3\sqrt{3}}\right)^{3/4} \cdot \left((k - 1/3)^{3/4} + \mathcal{O}(1/k^{3/4})\right)$$

as $k \to +\infty$.

4.2. Asymptotic analysis of the pole locations $\beta_k(t, \nu)$ as $\nu \to 0^+$ for fixed k and $t \neq t_*$. The saddle-point analysis of $E_\nu(i\beta, t)$ as $\nu \to 0^+$ in the case $t \neq t_*$ is very similar to the one that is described in [31]. There are, again, two equally relevant saddle points which come in a symmetric pair. Note that in this case, their positions are time dependent, and the steepest descent paths are very similar to those displayed in Fig. 4.1, except that the saddle points are either closer together or further apart depending on whether $t < t_*$ or $t > t_*$.

Let $w(z, i\beta) = i\beta z/t + \alpha z^2 - z^4$; $2\alpha = 1/t_* - 1/t < 0$ for $0 < t < t_*$. The saddle

points $z_s(\beta;t)$ are the roots of

$$0 = \frac{\partial w}{\partial z}(z, i\beta) = \frac{\beta}{t} i + 2\alpha z - 4z^3. \tag{4.6}$$

Throughout the remainder of the analysis, we write $(\beta;t)$ (as in $z_s(\beta;t)$) to denote that t is to be considered as a parameter. We let $z = -iu$; then u satisfies a cubic equation with real coefficients, namely,

$$u^3 + \frac{\alpha}{2} u - \frac{\beta}{4t} = 0.$$

In order to have some cancellation in the expansion of E_ν to obtain zeros, we need two equally relevant saddle points. Let $x_s(t) = t(2\alpha/3)^{3/2} = i\,(3t_*)^{-3/2}(t_* - t)^{3/2} t^{-1/2}$. Then for $t < t_*$, we find that two of the saddle points come in conjugate pairs only when $|\beta| > |x_s(t)|$, where $\beta = \pm|x_s(t)|$ is the boundary of analyticity of the inviscid solution up to $t = t_*$ (see [32, App. C]). From Cardan's formula for the roots of a cubic polynomial (see [32, App. B]), we find

$$\begin{cases} u_0 = \omega\mathcal{A} + \omega^2\mathcal{B} = -\frac{1}{2}\,(\mathcal{A}+\mathcal{B}) + i\frac{\sqrt{3}}{2}\,(\mathcal{A}-\mathcal{B})\,, \\ u_1 = \overline{u_0} = \omega^2\mathcal{A} + \omega\mathcal{B} = -\frac{1}{2}\,(\mathcal{A}+\mathcal{B}) - i\frac{\sqrt{3}}{2}\,(\mathcal{A}-\mathcal{B})\,, \\ u_2 = \mathcal{A} + \mathcal{B}, \end{cases} \tag{4.7}$$

where $\omega = e^{2\pi i/3}$. Since $x_s^2 = -|x_s^2| < 0$ for $t < t_*$, we find

$$\begin{cases} \mathcal{A}(\beta;t) = (8t)^{-1/3}\ \sqrt[3]{\beta + \sqrt{\beta^2 + x_s^2}} > 0 \\ \mathcal{B}(\beta;t) = (8t)^{-1/3}\ \sqrt[3]{\beta - \sqrt{\beta^2 + x_s^2}} > 0 \end{cases} \qquad \text{for } \boldsymbol{\beta > |x_s(t)|},$$

$$\begin{cases} \mathcal{A}(\beta;t) = -\,(8t)^{-1/3}\ \sqrt[3]{-\beta + \sqrt{\beta^2 + x_s^2}} < 0 \\ \mathcal{B}(\beta;t) = -\,(8t)^{-1/3}\ \sqrt[3]{-\beta - \sqrt{\beta^2 + x_s^2}} < 0 \end{cases} \qquad \text{for } \boldsymbol{\beta < -|x_s(t)|}, \tag{4.8}$$

so

$$z_s(-\beta;t) = -z_s(\beta;t). \tag{4.9}$$

Here we are taking the real positive branches of the square roots and cube roots in $\mathcal{A}$ and $\mathcal{B}$. We have also used the relation

$$|x_s\,(t)\,| = t\left(\frac{2|\alpha|}{3}\right)^{3/2} = t\left(-\frac{2\alpha}{3}\right)^{3/2} > 0, \tag{4.10}$$

where we are taking the positive branch of $z^{3/2}$ for $z > 0$. Moreover, when choosing the branches of the rational functions $\mathcal{A}$ and $\mathcal{B}$, one must make sure that they satisfy the relation $\mathcal{A}\cdot\mathcal{B} = -\alpha/6 > 0$ (see [32, App. B]). In terms of the original variable $z = -iu$, after separation of the real and imaginary parts, we have

$$\begin{cases} z_0 = \frac{\sqrt{3}}{2}(\mathcal{A}-\mathcal{B}) + \frac{i}{2}(\mathcal{A}+\mathcal{B}), \\ z_1 = -\overline{z_0} = \frac{\sqrt{3}}{2}(\mathcal{B}-\mathcal{A}) + \frac{i}{2}(\mathcal{A}+\mathcal{B}), \\ z_2 = -i(\mathcal{A}+\mathcal{B}). \end{cases} \tag{4.11}$$

Since we are only looking at values of $|\beta| > |x_s|$, the steepest paths and level curves look almost like the case $t = t_*$ described in Fig. 4.1 except that the saddle points have moved closer together, yet preserve the symmetry of Fig. 4.1. The path deformation is justified in the same way (see [31] for more details). The saddle points come in symmetric pairs that satisfy $z_0 = -\overline{z_1}$ for all $t > 0$. We have

$$0 = \frac{\partial w}{\partial z}\big(z_s(\beta;t), i\beta\big) = \frac{\beta}{t}i + 2\alpha z_s - 4z_s^3, \tag{4.12a}$$

$$0 = \frac{1}{4}z_s\frac{\partial w}{\partial z}\big(z_s(\beta;t), i\beta\big) = \frac{i\beta}{4t}z_s + \frac{\alpha}{2}z_s^2 - z_s^4, \tag{4.12b}$$

$$w\big(z_s(\beta;t), i\beta\big) = \frac{i\beta}{t}z_s + \alpha z_s^2 - z_s^4. \tag{4.12c}$$

Equation (4.12a) gives (4.12b), which combined with (4.12c) gives

$$w\big(z_s(\beta;t), i\beta\big) = \frac{3i\beta}{4t}z_s + \frac{\alpha}{2}z_s^2. \tag{4.13}$$

Since for $s = 0, 1$

$$z_s(\beta;t) = (-1)^s\frac{\sqrt{3}}{2}(\mathcal{A} - \mathcal{B}) + \frac{i}{2}(\mathcal{A} + \mathcal{B}), \tag{4.14a}$$

$$w_{zz}(z_s, i\beta) = 2\alpha - 12z_s^2, \quad w(z_0, i\beta) = \overline{w(z_1, i\beta)}, \tag{4.14b}$$

so

$$\Re\, w\big(z_s(\beta;t), i\beta\big) = \frac{\alpha}{4}(\mathcal{A}^2 + \mathcal{B}^2) - \frac{3\beta}{8t}(\mathcal{A} + \mathcal{B}) - \frac{\alpha^2}{6}, \tag{4.15a}$$

$$\Im\, w\big(z_s(\beta;t), i\beta\big) = (-1)^s\frac{\sqrt{3}}{8}\cdot(\mathcal{A} - \mathcal{B})\cdot(3\beta/t + 2\alpha(\mathcal{A} + \mathcal{B})), \tag{4.15b}$$

$$\theta(z_s(\beta;t), t) = \arg(-w_{zz}(z_s, i\beta)) = (-1)^s\arg(6z_0^2 - \alpha). \tag{4.15c}$$

Using a standard steepest descents analysis (see [31, 39] for example), we find that

$$E_\nu(i\beta, t) = \sum_{s=0,1}\sqrt{\frac{-4\pi\nu}{w_{zz}(z_s, i\beta)}}e^{w(z_s, i\beta)/2\nu}\,(1 + \mathcal{O}(\nu)) \quad \text{as } \nu \to 0^+.$$

We can further simplify the expansion using the actual value of $\sqrt{6z_s^2 - \alpha}$. Indeed, since $z_s(\beta;t) = (-1)^s\frac{\sqrt{3}}{2}(\mathcal{A} - \mathcal{B}) + \frac{i}{2}(\mathcal{A} + \mathcal{B}) = e^{i\pi/6}\mathcal{A} + e^{i5\pi/6}\mathcal{B}$ and $\mathcal{A}\cdot\mathcal{B} = -\alpha/6$,

$$6z_s^2 - \alpha = 3\sqrt{(\mathcal{A}^2 + \mathcal{B}^2 - \alpha)^2 + 3(\mathcal{A}^2 - \mathcal{B}^2)}\,e^{i\theta(z_s(\beta;t),t)}, \tag{4.16a}$$

$$\theta(z_s(\beta;t), t) = \arg(6z_s^2 - \alpha) = (-1)^s\,\tan^{-1}\left(\sqrt{3}\cdot\frac{\mathcal{A}^2 - \mathcal{B}^2}{\mathcal{A}^2 + \mathcal{B}^2 + \alpha/3}\right), \tag{4.16b}$$

where in (4.16b) we are taking the branch of $\tan^{-1}x$ for which $|\tan^{-1}x| < \pi/2$. Reproducing a similar analysis for $t > t_*$, we have the following result.

THEOREM 4.4. *The asymptotic expansion of $E_\nu(i\beta, t)$ as $\nu \to 0^+$ is*

$$E_\nu(i\beta, t) = \sqrt{\frac{2\pi\nu}{|6z_s^2 - \alpha|}}\exp\left\{\frac{1}{2\nu}\,\Re\, w\big(z_s(\beta;t), i\beta\big)\right\} \times\left[\cos\Big(\frac{1}{2\nu}\,\Im\, w\big(z_0(\beta;t), i\beta\big) - \frac{1}{2}\theta(z_0(\beta;t), t)\Big) + \mathcal{O}(\nu)\right],$$

where

$$z_s(\beta;t) = (-1)^s \frac{\sqrt{3}}{2}(\mathcal{A}-\mathcal{B}) + \frac{i}{2}(\mathcal{A}+\mathcal{B}) \qquad \textit{for } s=0,1,$$

and $\mathcal{A}$ *and* $\mathcal{B}$ *are given by*

$$\mathcal{A}(\beta;t) = (8t)^{-1/3}\ \sqrt[3]{\beta+\sqrt{\beta^2+x_s^2}}$$

$$\mathcal{B}(\beta;t) = \begin{cases} 0<t<t_* & (8t)^{-1/3}\ \sqrt[3]{\beta-\sqrt{\beta^2+x_s^2}} > 0 \qquad \beta > |x_s|, \\ t>t_* & -(8t)^{-1/3}\ \sqrt[3]{-\beta+\sqrt{\beta^2+x_s^2}} < 0 \qquad \beta > 0. \end{cases}$$

For $\beta < 0$, $z_s(\beta;t)$ is defined by the odd parity condition $z_s(\beta;t) = -z_s(-\beta;t)$. Letting $t \to t_*$ in Theorem 4.4, we obtain $\theta(z_s(\beta;t_*),t_*) = (-1)^s\pi/3$, and

$$\Re\, w\big(z_s(\beta;t_*), i\beta\big) = -\frac{3}{2}\left(\frac{\beta}{4t_*}\right)^{4/3},$$

$$\Im\, w\big(z_s(\beta;t_*), i\beta\big) = (-1)^s \frac{3\sqrt{3}}{2}\left(\frac{\beta}{4t_*}\right)^{4/3}.$$

For small ν, the poles β_k are approximated by the roots of the equation

$$\frac{1}{2\nu}\,\Im\, w\big(z_0(\beta;t), i\beta\big) - \frac{1}{2}\theta(z_0(\beta;t),t) = \left(k-\frac{1}{2}\right)\pi, \quad k\in\mathbb{N}^*, \tag{4.17}$$

with the convention that $\beta_{-k} \equiv -\beta_k$. Since $|\theta(z_0(\beta_k;t),t)| < \pi$ for all $\beta_k \in \mathbb{R}$, the limiting behavior of the poles is given by $\Im\, w\big(z_0(\beta;t), i\beta\big) = 0$. Recall from (4.15b) that

$$\Im w_s = \Im\, w\big(z_s(\beta;t), i\beta\big) = (-1)^s \frac{\sqrt{3}}{8}\cdot(\mathcal{A}-\mathcal{B})\cdot(3\beta/t + 2\alpha(\mathcal{A}+\mathcal{B})),$$

so

$$\Im w_s = 0 \Leftrightarrow \begin{cases} \text{either } \mathcal{A}=\mathcal{B} \text{ or} \\ 3\beta/t + 2\alpha(\mathcal{A}+\mathcal{B}) = 0. \end{cases} \tag{4.18}$$

For $0<t\le t_*$, $\alpha \le 0$: if $\beta \ge |x_s|$ then $\mathcal{A}>0$, $\mathcal{B}>0$; if $\beta \le |x_s|$ then $\mathcal{A}<0$, $\mathcal{B}<0$. We rewrite the second equation as $(\mathcal{A}+\mathcal{B})^3 = -(3\beta/2\alpha t)^3$, which, after expanding the left-hand side and using the fact that $\mathcal{A}\cdot\mathcal{B} = -\alpha/6$, reduces to $\beta = \pm|x_s(t)|$. The same conclusion is reached from the first equation $\mathcal{A}=\mathcal{B}$. Thus, for $0<t\le t_*$, $\Im w_s = 0$ only if $\beta = \pm|x_s|$. Let $\hat\beta \ll \beta$. Then, re-substituting $\beta = |x_s(t)| + \hat\beta$ into the expansion for $E_\nu(i\beta,t)$ in Theorem 4.4 and reproducing an analysis which is similar to the one described in [31] (i.e., inverting the asymptotic series expansion), we find that the error term is $\mathcal{O}((k\nu)^{3/4})$ as $\nu\to 0^+$ for fixed k. Thus, we can write that $\beta_{\pm k}(t,\nu) = \pm|x_s| + \mathcal{O}((k\nu)^{3/4})$ as $\nu\to 0^+$ for fixed k. Similarly, for $t\ge t_*$, $\alpha\ge 0$, $\beta>0 \Rightarrow \mathcal{A}-\mathcal{B}>0$ and $\beta<0 \Rightarrow \mathcal{A}-\mathcal{B}<0$; hence, $\Im w_s = 0 \Leftrightarrow \beta = 0$ as a result of setting $3\beta/t + 2\alpha(\mathcal{A}+\mathcal{B}) = 0$. Since $\Im x_s(t) = 0$ for $t\ge t_*$, we have proved the following (see Fig. 5.12).

COROLLARY 4.5. *For all* $t>0$ *and fixed* k*, the asymptotic behavior of the poles* $x = \pm a_k(t,\nu) = \pm i\beta_k(t,\nu)$ *is given by*

$$\beta_k(t,\nu) = \Im x_s(t) + \mathcal{O}((k\nu)^{3/4}) \qquad \textit{as } \nu\to 0^+.$$

Since $\Im x_s(t) = 0$ *for* $t \geq t_*$,

$$\beta_k(t,\nu) = \mathcal{O}((k\nu)^{3/4}) \qquad \text{as } \nu \to 0^+$$

for fixed k. *Of particular interest is the modulus of the first ordered pole* $\beta_1(t,\nu)$ *which governs the time evolution of the width of the analyticity strip of the viscous solution.*

Following the exact same steps in the proof of Corollary 4.5, one can show the following corollary.

COROLLARY 4.6. *For all* $t > 0$ *and fixed* ν, *the asymptotic behavior of the poles* $x = \pm a_k(t,\nu) = \pm i\beta_k(t,\nu)$ *is*

$$\beta_k(t,\nu) = \mathcal{O}((k\nu)^{3/4}) \qquad \text{as } k \to +\infty.$$

5. Numerics.

5.1. Finite difference approximation, asymptotic approximation, and pole expansion. We present a numerical scheme which enables us to solve (1.1) for moderately small values of ν. The procedure is sometimes referred to as the method of lines and consists in using a centered difference operator in space while time-marching with a Runge–Kutta scheme. The method is implemented on the interval $I = [0, 1/2]$ with boundary conditions

$$u_\nu(0,t) = u_\nu(1/2,t) = 0. \tag{5.1}$$

The boundary condition $u_\nu(1/2,t) = 0$ is chosen to be consistent with the value of the inviscid solution $u(1/2,t) = 0$. Thus, we can expect the difference approximation to be consistent with the initial (boundary) value problem for small ν. Two different initial conditions are also used:

$$u(x,0) = u_\nu(x,0) = 4x^3 - \frac{x}{t_*}, \tag{5.2a}$$

$$u_\nu(x,t_*) = \frac{x}{t_*} - \sum_{n=1}^{\infty} \frac{4\nu x}{x^2 + \beta_n^2(t_*,\nu)}. \tag{5.2b}$$

Throughout the numerics we use the parameter value $t_* = 1$. If the second condition is used, then the pole positions at $t = t_*$ are specified by the asymptotic estimate presented in Theorem 4.2. This estimate is used for all values of μ_n for $10 \leq n \leq N$:

$$\begin{cases} \beta_n(t_*,\nu) = 4t_*(2\nu\mu_n)^{3/4}, \\ \mu_n = G(\mu_n^{(0)}), \quad \mu_n^{(0)} = \frac{2\pi}{3\sqrt{3}}(n - 1/3), \quad n \geq 10, \\ G(\mu) = \mu + \frac{7}{432\mu}\left(1 - \frac{1}{6\mu}\left(1 + \frac{7}{72\mu}\left(1 - \frac{5}{12\mu}\left(1 + \frac{53143}{18900\mu}\right)\right)\right)\right). \end{cases} \tag{5.3}$$

For $1 \leq n \leq 9$, we use the numerical values found in [31, Table 3], under the column "Numerical roots":

$$\mu_1 = 0.8221037147, \quad \mu_2 = 2.0226889660, \quad \mu_3 = 3.2292915284, \tag{5.4}$$

$$\mu_4 = 4.4372464748, \quad \mu_5 = 5.6457167459, \quad \mu_6 = 6.8544374340, \tag{5.5}$$

$$\mu_7 = 8.0632985369, \quad \mu_8 = 9.2722462225, \quad \mu_9 = 10.4812510479. \tag{5.6}$$

Let

$$u_j = u_\nu(j * \Delta x, t), \quad Ev_j = v_{j+1}, \quad E^p v_j = v_{j+p},$$
$$D_+ = (E - E^0)/\Delta x, \quad D_- = (E^0 - E^{-1})/\Delta x, \quad D_0 = (D_+ + D_-)/2.$$

One then solves the system of $N_x - 1$ equations using a Runge–Kutta 4–5 scheme (which we refer to as RK45):

$$\begin{cases} du_j/dt = -D_0(u_j^2/2) + \nu D_+ D_- u_j, \quad j = 1, \dots, N_x - 1, \\ u_{j=0} = u_\nu(0,t) = 0, \quad u_{j=N_x} = u_\nu(1/2,t) = 0, \end{cases} \tag{5.7}$$

where N_x is the number of gridpoints (and gridfunctions) and $N_x * \Delta x = 1/2$. Typically, the mesh size we use is $\Delta x = .25 \times 10^{-2}$ and $N_x = 200$ gridpoints. The time stepping restrictions depend on the size of ν and on how far in time one wants to go. For example, if the final time is $t = t_* = 1$, whether $\nu = 10^{-2}$ or $\nu = 10^{-3}$ it suffices to use $\Delta t = .25 \times 10^{-2}$, $N_t = 400$ RK45 steps. However, for $\nu = 10^{-2}$, if one wants to go as far as $t = 2$, for reasons of stability one needs to use a smaller time step such as $\Delta t = 10^{-3}$, $N_t = 2,000$. The domain of integration is $(x,t) \in [0,1/2] \times [0,T]$, where $T = 1$ or $T = 2$. Then, due to the odd parity of the solution, we reflect symmetrically for $x \in [-1/2, 0]$ according to the rule $u_\nu(-x,t) = -u_\nu(x,t)$. This finite difference scheme is used in order to compare the predictions obtained from the pole expansion and the pole dynamics in section 5.2.

5.2. Numerical pole dynamics. We investigate the motion of the simple poles of $u_\nu(x,t)$ by solving the truncated CDS and by starting with initial data for the poles at $t = t_*$. The poles of $u_\nu(x,t)$ are located at $\pm a_n(t,\nu) = \pm i\sqrt{\nu\gamma_n(t,\nu)}$, where the variables $\gamma_n(t,\nu) > 0$ satisfy the system (cf. Property 2.2)

$$\begin{cases} \dfrac{\dot\gamma_n}{2} = \dfrac{\gamma_n}{t} + 1 - 4\,\gamma_n \sum_{l \neq n} \dfrac{1}{\gamma_l - \gamma_n} \qquad \forall n \in \mathbb{N}. \\ \gamma_n(t_*,\nu) = (4t_*)^2\,(2\mu_n)^{3/2}\,\sqrt{\nu} \end{cases} \tag{5.8}$$

In order to solve this system we use the asymptotic estimate for μ_n presented in (5.3) and the numerical values of (5.5). We are mainly interested in describing the motion of the first pole $a_1(t,\nu) = i\beta_1(t,\nu) \in i\mathbb{R}$; this amounts to describing the time evolution of the width of the strip of analyticity of the solution $u_\nu(t,x)$. The imaginary part of the poles $\beta_n(t,\nu)$ is recovered using the relation $\beta_n(t,\nu) = \sqrt{\nu\gamma_n(t,\nu)}$. We plot the evolution of $\beta_n(t,\nu), n = 1, \dots, 4$ for different values of ν. We use N poles in the computations, i.e., β_1 through β_N where $N \times 10^{-4}$ varies from $.1, .5, 1, 2.5, 5$. That is, we consider the truncated system

$$\begin{cases} \dfrac{\dot\gamma_n}{2} = \dfrac{\gamma_n}{t} + 1 - 4\gamma_n \sum_{\substack{l=1 \\ l \neq n}}^{N} \dfrac{1}{\gamma_l - \gamma_n} \qquad \forall n = 1, \dots, N. \\ \gamma_n(t_*,\nu) = (4t_*)^2 (2\mu_n)^{3/2} \sqrt{\nu} \end{cases}$$

In order to accelerate the computation of the slowly converging pole expansions which require $\mathcal{O}(N^2)$ operations

$$\sum_{\substack{l=1 \\ l \neq n}}^{N} \frac{1}{\gamma_l - \gamma_n} \qquad \forall n = 1, \dots, N, \tag{5.9}$$

we use a multipole algorithm developed and implemented by Greengard and Rokhlin [14, 21] which reduces the computational complexity to $\mathcal{O}(N \log N)$. A fourth/fifth-order Runge–Kutta–Fehlberg scheme with automatic step-size control is used (the same one that is used for the finite difference scheme/method of lines computations

of the previous section). Since the initial data is specified at $t = t_* = 1$, we can solve the system forward and backwards in time starting from $t = 1$. The typical bound on the relative error in the computation is $10^{-8} < |(x_4 - x_5)/x_5| < 10^{-4}$, where x_4 and x_5 are, respectively, the 4th- and 5th-order estimates of $\gamma_1(t, \nu)$. Once this error criterion is met, we recover the pole location via the relation $a_n(t, \nu) = i\sqrt{\nu\gamma_n(t, \nu)}$. The justification of the numerics is the most difficult aspect of this simulation because one must justify the convergence of the method as both the number of poles increases and the time step is refined. The time-step control is automatically determined by the local relative tolerance (LRT $= |(x_4 - x_5)/x_5|$) test on the 4th- and 5th-order approximations of the first ordered pole (the one closest to the origin). Thus, one cannot fix the time stepping; rather, one can have a subtle control on it by reducing this tolerance. Typically, we fix the number of poles to $N = 50,000$ and vary the tolerance on the successive intervals $10^{-10} < LRT < 10^{-6}$, $10^{-8} < LRT < 10^{-4}$, and $10^{-6} < LRT < 10^{-2}$. Then we fix the tolerance at the highest reasonable level $10^{-8} < LRT < 10^{-4}$ and vary the number of poles where $N \times 10^{-4}$ is either $.1, .5, 1, 2.5$, or 5. We see that the time step barely affects the convergence of the method. Thus, the main difficulty in this procedure arises from the slow convergence of the pole interaction (5.9) that is present in the CDS.

5.2.1. Exact solution for the two-pair pole-dynamics test. In order to verify the accuracy of the numerical pole dynamics, we implement the numerical method described in the previous section for the case where there are only four poles (two pairs). In this case, one can explicitly solve the resulting system as follows: let $a_n = i\beta_n$. That is, replace β_n by $-ia_n$ in Property 2.2 so that the two pairs of poles $\{(-a_1, a_1), (-a_2, a_2)\}$ and $\{(-\kappa_1, \kappa_1), (-\kappa_2, \kappa_2)\}$ satisfy, under the transformation $\kappa_n = a_n^2/\nu$, the equivalent systems

$$\begin{cases} \dot{a}_1 = a_1/t - \nu/a_1 - 4\nu a_1/(a_1^2 - a_2^2), \\ \dot{a}_2 = a_2/t - \nu/a_2 + 4\nu a_2/(a_1^2 - a_2^2), \end{cases} \iff \begin{cases} \dot{\kappa}_1/2 = \kappa_1/t - 1 - 4\kappa_1/(\kappa_1 - \kappa_2), \\ \dot{\kappa}_2/2 = \kappa_2/t - 1 + 4\kappa_2/(\kappa_1 - \kappa_2). \end{cases}$$

Introduce a set of new variables $\{\Theta_1,\Theta_2\}$ defined by

$$\begin{cases} \Theta_1 = \kappa_1 + \kappa_2, \\ \Theta_2 = \kappa_1 - \kappa_2, \end{cases} \iff \begin{cases} \kappa_1 = (\Theta_1 + \Theta_2)/2, \\ \kappa_1 = (\Theta_1 - \Theta_2)/2. \end{cases}$$

Then it is easy to show that $\{\Theta_1,\Theta_2\}$ satisfy the coupled system of nonlinear ODEs

$$\begin{cases} \dot{\Theta}_1 - 2\Theta_1/t = -12, \\ \dot{\Theta}_2 - 2\Theta_2/t = -8\Theta_1/\Theta_2. \end{cases} \tag{5.10}$$

We further introduce a new variable denoted by $\phi_2 = \Theta_2^2$ which in turn satisfies the linear ODE

$$\dot{\phi}_2 - 4\phi_2/t = -16\Theta_1. \tag{5.11}$$

We use as initial data the position of the poles $a_1(t_*, \nu) = i\beta_1(t_*, \nu)$ and $a_2(t_*, \nu) = i\beta_1(t_*, \nu)$, where $\beta_1(t_*, \nu)$ and $\beta_2(t_*, \nu)$ are given in (5.3) and (5.4). Thus, we have

$$\begin{cases} \Theta_1^* = \Theta_1(t_*, \nu) = \kappa_1(t_*, \nu) + \kappa_2(t_*, \nu) = a_1^2(t_*, \nu)/\nu + a_2^2(t_*, \nu)/\nu, \\ \phi_2^* = \phi_2(t_*, \nu) = \Theta_2^2(t_*, \nu) = (a_1^2(t_*, \nu)/\nu - a_2^2(t_*, \nu)/\nu)^2. \end{cases} \tag{5.12}$$

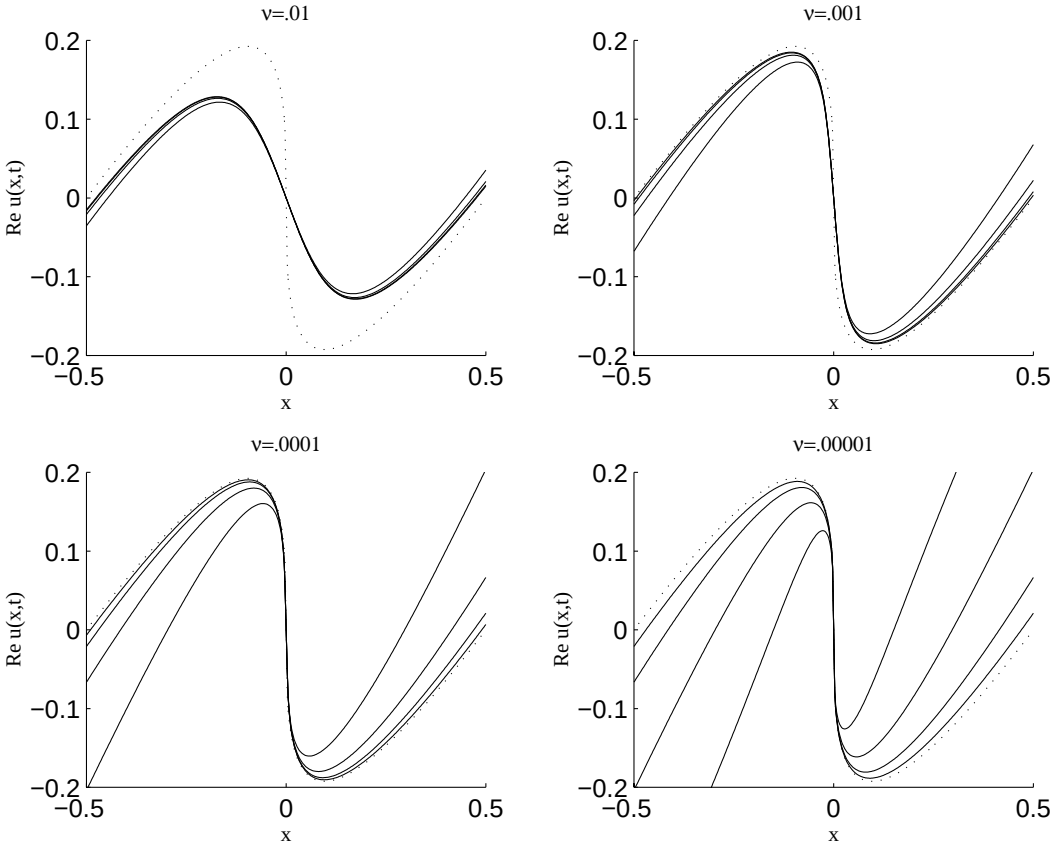

FIG. 5.1. *Convergence of the pole expansion as* $N \to +\infty$ *of the solution* $u_\nu(x,t_*) = x/t_* - \Sigma_{n=1}^{N} 4\nu x/(x^2+\beta_n^2(t_*,\nu))$ *with varying number of poles ranging from* $N = 10^3, 10^4, 10^5, 10^6$ *poles for* $\nu = 10^{-2}, 10^{-3}, 10^{-4}, 10^{-5}$. *The dotted curve is computed from the inviscid solution at* $t = t_* = 1$ *by* $u(x,t_*) = x/t_* - (x/4t_*)^{1/3}$. *For* $\nu = 10^{-2}$, *the inviscid solution and the pole expansion* $u_\nu(x,t_*)$ *do not agree because the viscosity is large enough that the solution has started decaying earlier (see comments on the turn-around time of the poles and their relation to the decay of the solution).*

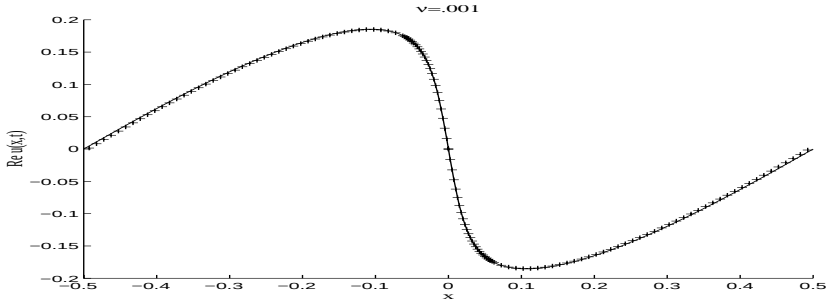

FIG. 5.2. *Comparison of the solution reconstruction at* $t = t_* = 1$ *from the pole expansion* $u_\nu(x,t_*) = x/t_* - \Sigma_{n=1}^{N} 4\nu x/(x^2+\beta_n^2(t_*,\nu))$ *with* $N = 10^6$ *poles and the finite difference scheme (method of lines) for* $\nu = 10^{-3}$. *Mesh size:* $N_x = 200$ *points,* $\Delta x = .25 * 10^{-2}$, $N_t = 400$ *RK*45 *time steps with* $\Delta t = .25 * 10^{-2}$. *Pole expansion* $(+)$ *at* $t = 1$ *overlaps finite difference approximation in solid curve.*

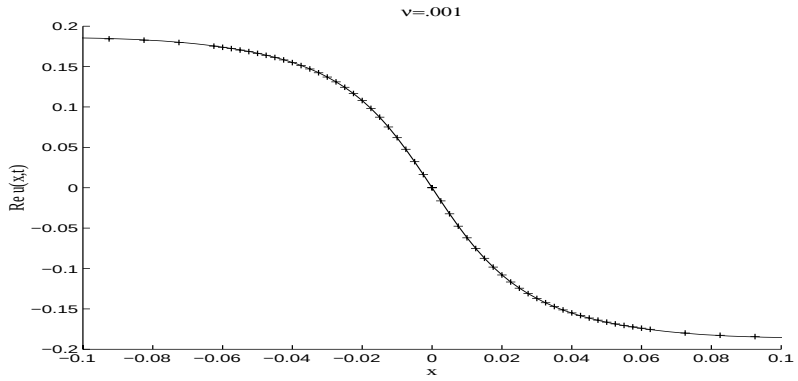

FIG. 5.3. *Closeup of Fig.* 5.2 *in* $[-.1, .1]$.

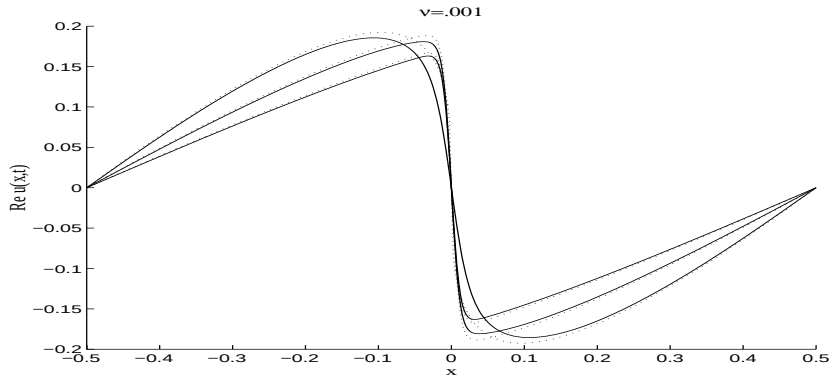

FIG. 5.4. *Comparison of finite difference scheme and saddle-point method for* $\nu = 10^{-3}$ *at* $t = 1, 1.5, 2$. *Solid curves: finite difference scheme with* $N_x = 200$ *points,* $\Delta x = .25 * 10^{-2}$, $N_t = 800$ *RK*45 *time steps with* $\Delta t = .25 * 10^{-2}$. *Dotted curves: saddle-point approximation overshooting the finite difference approximation.*

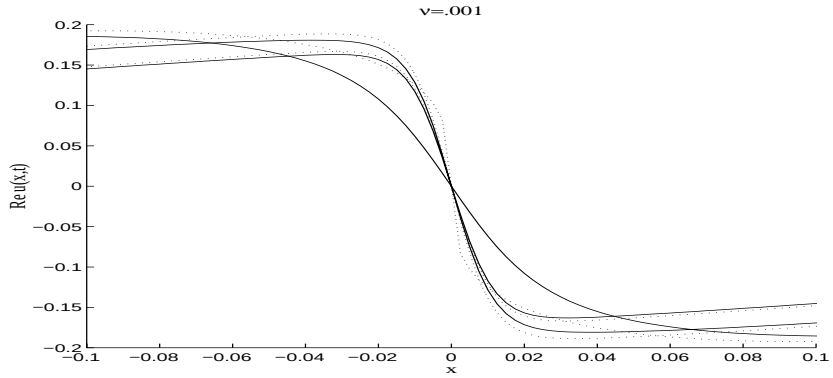

FIG. 5.5. *Closeup of Fig.* 5.4 *in* $[-.1, .1]$.

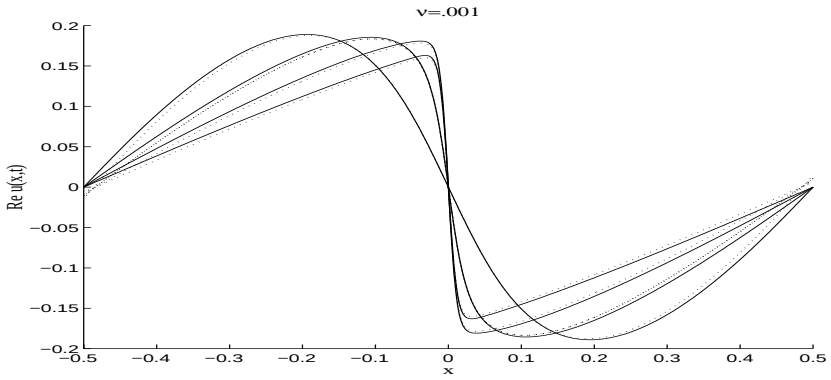

FIG. 5.6. *Comparison of the finite difference approximation (solid) and the pole dynamics (dotted) for* $\nu = 10^{-3}$ *at* $t = .5, 1, 1.5, 2$. *Finite difference mesh size:* $N_x = 200$ *points,* $\Delta x = .25 * 10^{-2}$, $N_t = 2,000$ *RK*45 *steps with* $\Delta t = .5 * 10^{-2}$. *Pole dynamics:* $N = 5 * 10^4$ *poles,* $10^{-8} < LRT < 10^{-4}$, *typical time step* $\Delta t = .05$, $N_t = 45$ *RK*45 *time steps (*25 *steps backward and* 20 *steps forward from* $t = t_*$*).*

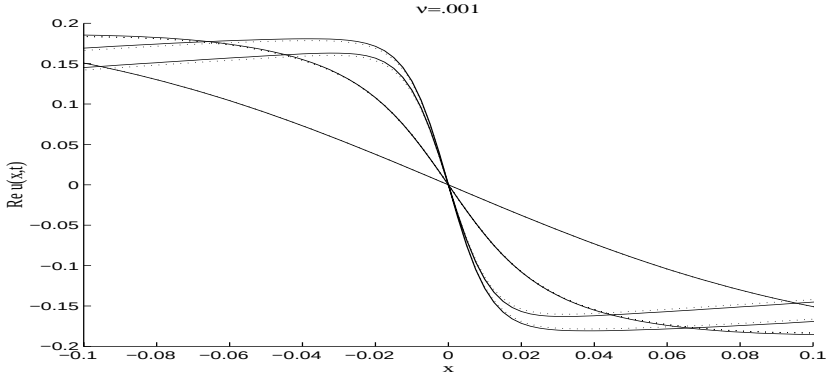

FIG. 5.7. *Closeup of Fig.* 5.6 *in* $[-.1, .1]$.

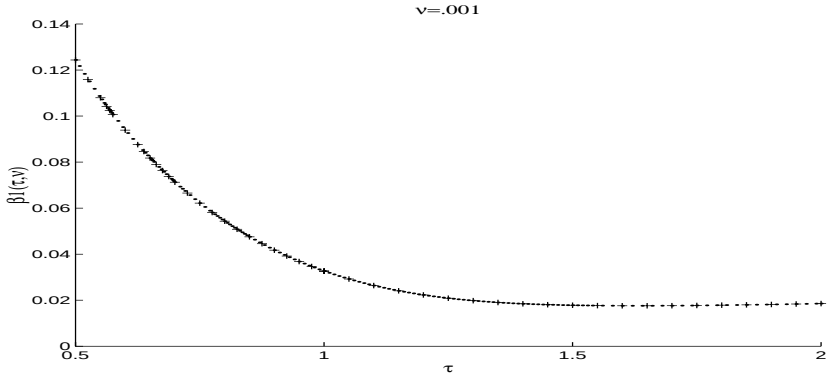

FIG. 5.8. $\beta_1(t, \nu)$ *vs.* t. *Time evolution in* $\mathbb{R}$ *of the width of the analyticity strip* $\beta_1(t, \nu)$ *for* $\nu = 10^{-3}$ *and* $N = 5 \times 10^4$ *poles.* $t_{initial} = t_* = 1$ *and* $t \in [.5, 2]$. *(+):* $\Delta t = .05$*; dots (.):* $\Delta t = .01$. *Both curves are indistinguishable.*

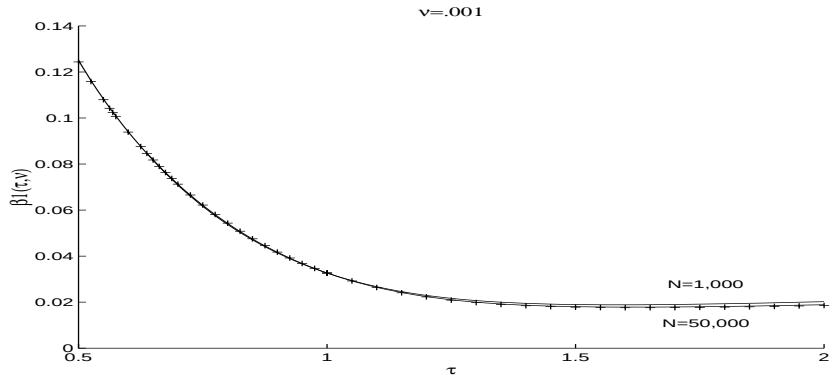

FIG. 5.9. *Closeup of Fig.* 5.8 *for* $t \in [1, 2]$.

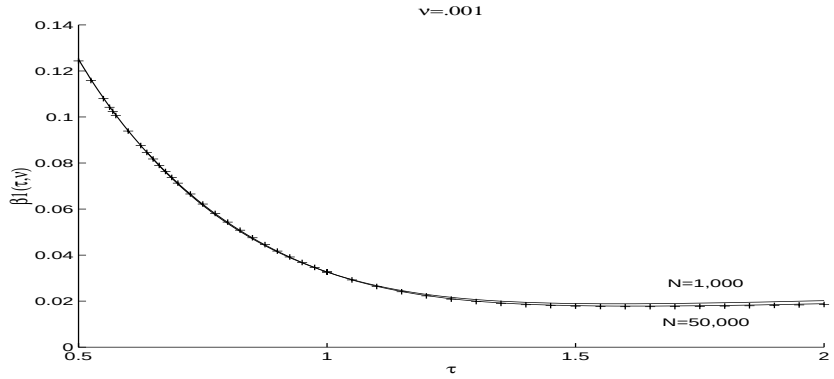

FIG. 5.10. $\beta_1(t, \nu)$ *vs.* t. *Comparison of pole number simulations for* $\nu = 10^{-3}$ *and* $N = .1, .5, 1, 2.5, 5 \times 10^4$ *poles. (+):* $N = 5 \times 10^4$ *poles; (solid):* $N = .1, .5, 1, 2.5 \times 10^4$ *poles. Differences appear more clearly in the closeup in Fig.* 5.11.

Solving the IVP consisting of the first equation in system (5.10) and equations (5.11) and (5.12), we find that

$$\begin{cases} \Theta_1(t, \nu) = (t/t_*)^2 \Theta_1^* - 12t(t - t_*)/t_*, \\ \phi_2(t, \nu) = (t/t_*)^4 \left(\phi_2^* - 16 t_* (t - t_*)(t\Theta_1^* - 6tt_* + 6t_*^2)/t^2 \right). \end{cases} \tag{5.13}$$

Taking $t_* = 1$, $\nu = .001$, we use (5.13), a straightforward numerical integration scheme using RK45 and RK45 together with the multipole algorithm in which we set to zero all coefficients pertaining to $a_n, n \geq 3$. We find common values for all three methods at $t = 1.25$:

$$\begin{cases} a_1(t = 1.25, \nu = .001) = 0.0408023705 * i, \\ a_2(t = 1.25, \nu = .001) = 0.1009178717 * i. \end{cases} \tag{5.14}$$

Computing the differences between the exact values of a_1 and a_2 and the predictions obtained from the Runge–Kutta schemes (with and without the multipole algorithm), we find that these predictions are of the order of $\mathcal{O}(10^{-10})$, which is consistent with the expected 4th-order accuracy of such numerical schemes.

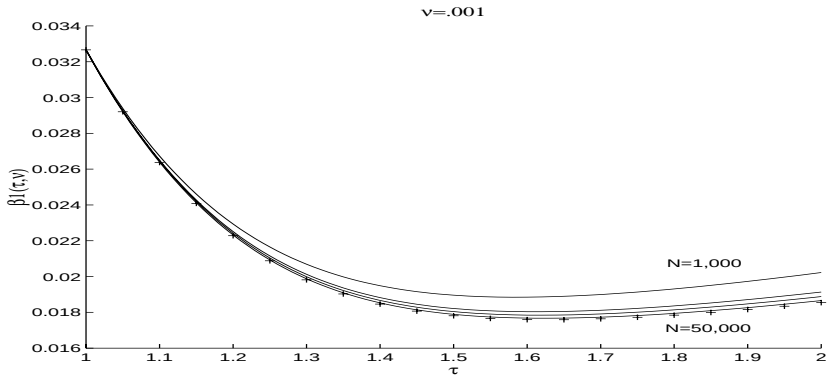

FIG. 5.11. *Closeup of Fig.* 5.10 *for* $t \in [1,2]$. *Turn-around time at* $t_u \approx 1.62$.

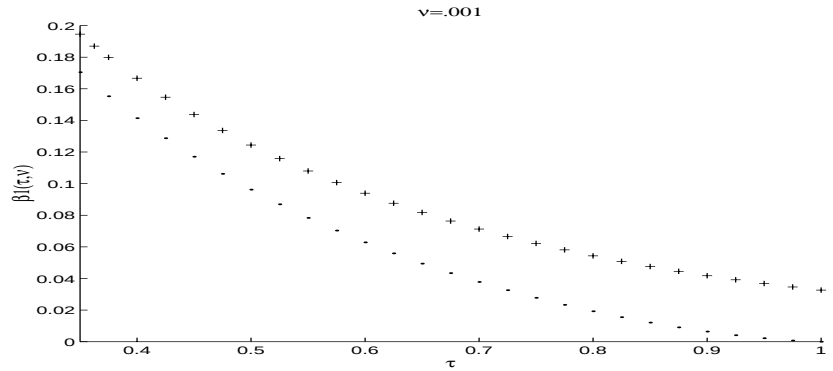

FIG. 5.12. *Comparison of the time evolutions of* $\beta_1(t, \nu = 10^{-3})$ (+) *and* $x_s(t)$ (.) *for* $t \in [.35, t_* = 1]$. *The pole dynamics are the same as Fig.* 5.8 *with* $N = 5 \times 10^4$ *poles. This illustrates the asymptotic relation* $\beta_1(t,\nu) = \Im x_s(t) + \mathcal{O}(\nu^{3/4})$ *as* $\nu \to 0^+$ *when* $t \le t_*$ *(see Corollary* 4.5*).*

5.3. Figures, descriptions, and comparisons. In Fig. 5.1, we illustrate the "slow" convergence of the pole expansion as the viscosity decreases. In particular, for $\nu = 10^{-4}$ and 10^{-5}, we can compare the inviscid solution given by (see [32, App. C])

$$u(x,t_*) = \frac{x}{t_*} - \left(\frac{x}{4t_*}\right)^{1/3} \tag{5.15}$$

to the pole expansion and expect good agreement between the two. For ν very small, we see that even for a very large number of poles ($N = 10^6$) the tails of the pole expansion still do not match the true solution, which is expected to be very close to the inviscid one. In each of these figures there are five curves, four of which are computed from the pole expansion for an increasing number of poles $N = 10^3, 10^4, 10^5, 10^6$. The fifth (dotted curve) is the inviscid solution at t_*.

In Figs. 5.2 and 5.3 we present comparisons between the finite difference scheme and the pole expansion ($N = 10^6$ poles) at the fixed time t_*. For the finite difference scheme, we use $N_x = 200$ points, $\Delta x = .25 * 10^{-2}$, $N_t = 400$ RK45 steps with $\Delta t = .25 * 10^{-2}$.

In Figs. 5.4 and 5.5 we present comparisons between the finite difference scheme

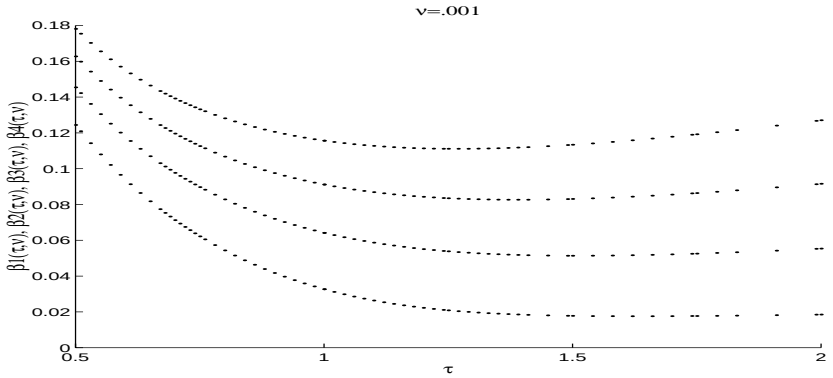

FIG. 5.13. *$\beta_j(t,\nu)$ vs. t for $j = 1,\dots,4$. $\nu = 10^{-3}$ and $N = 5\times 10^4$ poles. Same parameters as in Fig. 5.8. Turn-around times at $t_u \approx 1.62$, $t_u \approx 1.51$, $t_u \approx 1.39$, $t_u \approx 1.27$ for $\beta_j(t,\nu), j = 1,\dots,4$.*

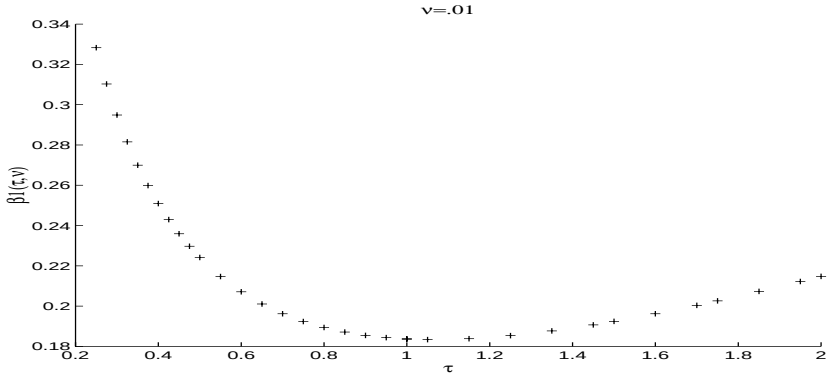

FIG. 5.14. *$\beta_1(t,\nu)$ vs. t. Time evolution in $\mathbb{R}$ of the width of the analyticity strip $\beta_1(t,\nu)$ for $\nu = 10^{-2}$ and $N = 5\times 10^4$ poles. $t_{initial} = t_* = 1$ and $t \in [.25, 2]$. $N_{steps} = 32$ (20 steps backward and 12 steps forward from $t = t_*$). Local relative tolerance: $10^{-10} < LRT < 10^{-6}$.*

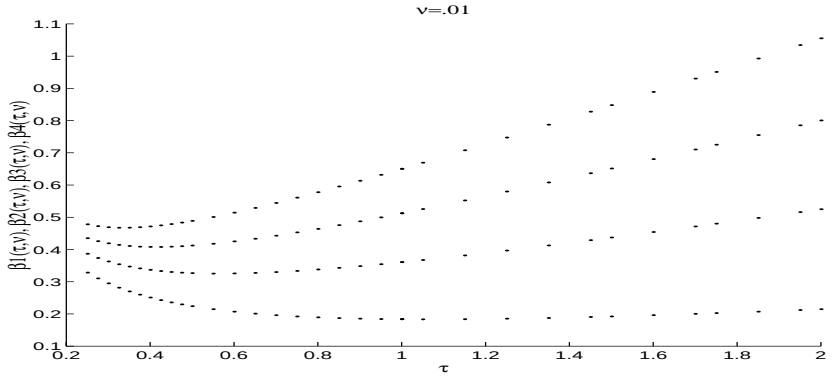

FIG. 5.15. *$\beta_j(t,\nu)$ vs. t for $t \in [.25, 2]$ and $j = 1,\dots,4$. $\nu = 10^{-2}$ and $N = 5\times 10^4$ poles. Same parameters as in Fig. 5.14. Turn around times at $t_u \approx 1.05$, $t_u \approx .55$, $t_u \approx .425$, $t_u \approx .325$ for $\beta_j(t,\nu), j = 1,\dots,4$.*

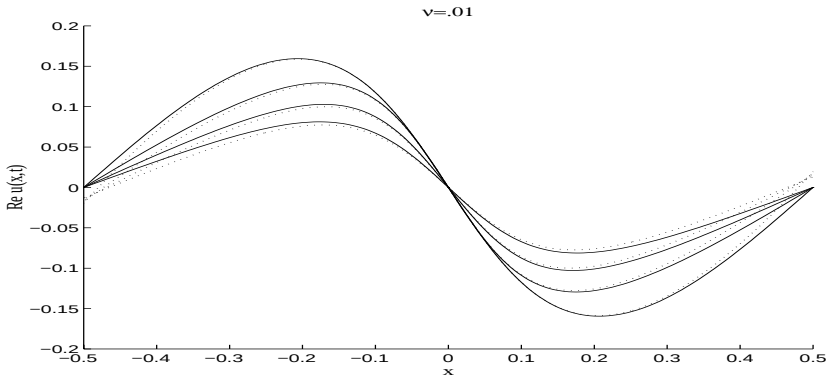

FIG. 5.16. *Comparison of the finite difference approximation (solid) and the pole dynamics (dotted) for* $\nu = 10^{-2}$ *at* $t = .5, 1, 1.5, 2$. *Finite difference mesh size:* $N_x = 100$ *points,* $\Delta x = .5 * 10^{-2}$, $N_t = 2,000$ *RK45 time steps with* $\Delta t = 10^{-3}$. *Pole dynamics: same as Fig.* 5.14.

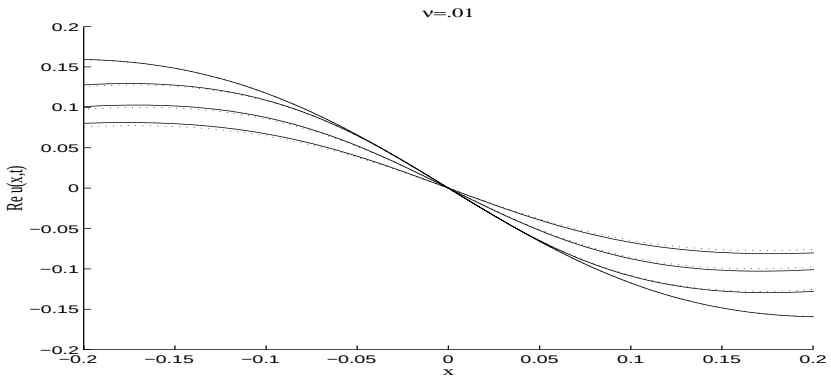

FIG. 5.17. *Closeup of Fig.* 5.6 *in* $[-.2, .2]$.

and the saddle-point approximation at the successive times $t = 1, 1.5, 2$. The mesh size is the same as the one for Figs. 5.2 and 5.3. One can observe that the saddle-point approximation overshoots the true value of the solution which is best captured by the difference scheme. This overshoot is due to the degeneracy of the saddle-point formula at the caustic and the inaccuracies around it. The correct behavior in a neighborhood of this caustic can be correctly described only by the uniform asymptotic expansion of section 3.3.

In Figs. 5.6 and 5.7, we compare the difference method and the pole dynamics for $\nu = 10^{-3}$ with $N = 50,000$ poles at the times $t = .5, 1, 1.5, 2$. The pole dynamics are run forward and backward in time starting from $t = t_* = 1$ until $t = .5$ and $t = 2$. The solution is then reconstructed from the pole expansion and the pole locations at these specific times and is compared to the finite difference approximations with mesh size $N_x = 200$ points, $\Delta x = .25 * 10^{-2}$, $N_t = 2,000$ RK45 time steps with $\Delta t = 10^{-3}$. The agreement between the finite difference and the pole dynamics close to the shock region is very good as opposed to the tails. Since the pole dynamics simulation involved only $50,000$ poles in Fig. 5.6, the mismatch in the tail is characteristic of the slow convergence of the pole expansion in the tails that are displayed in Fig. 5.1 for

$\nu = 10^{-3}$. There is also a small source of error in the difference scheme where the boundary condition at $x = 1/2$ is set to the inviscid value ($u(1/2, t) = 0$). This error in the difference approximation increases for larger ν. Thus, the discrepancy observed in the tails of the solution in Fig. 5.16 is more likely to arise from errors in the difference scheme than the pole dynamics. Indeed, it suffices to look at the convergence of the pole expansion at $t = t_*$ in Fig. 5.1, $\nu = 10^{-2}$, to establish confidence in the pole dynamics.

However, one can notice that regardless of the size of ν (whether $\nu = 10^{-2}$ or 10^{-3}), within the shock region of width $\mathcal{O}(\nu)$, the agreement between the pole dynamics and the difference approximation is very good (see Figs. 5.3, 5.17). This shows that the dynamics of the first few poles is accurately captured by the pole dynamics. This also becomes apparent when comparing the simulations done with varying number of poles (see Figs. 5.10 and 5.11). Finally, it should be noted that increasing the step-size of the time increment (in a reasonable way) in the pole dynamics barely affects the computations (see Figs. 5.8 and 5.9).

We plot the evolution of the first four (ordered) poles on the imaginary axis ($\beta_k, k = 1, \dots, 4$) and focus on the "turn-around" times t_u and the position of the first ordered pole β_1, which determines the width of the analyticity strip. One can see that the behavior of the pole β_1 displayed in Figs. 5.8 and 5.14 is qualitatively similar to the one obtained by Sulem, Sulem, and Frisch in [35, section III-B, Fig. 3] using spectral methods for the initial data $u_0(x) = \sin(x)$ with $\nu = .05$. The most important feature in the behavior of the first ordered pole is clearly the fact that it turns around before crossing the real axis, thus preserving the uniform analyticity of the viscous solution within the strip $|\Im x| \leq \delta_1 < \beta_1$, where $\beta_1(t, \nu) > 0$ for all $t > 0$. Moreover, it is interesting to note that the poles $\pm\beta_k(t, \nu)$ are confined to the imaginary axis and move towards the origin until a time $t = t_u(k)$, $k \in \mathbb{Z}^*$; this is the time at which they turn around and move away from the origin. These turn-around times $t_u(k)$ decrease as k increases: $t_u(1) > t_u(2) > \cdots > t_u(n) > \cdots > 0$. Moreover, $t_u(1)$ occurs before t_* for $\nu \gtrapprox .01$ and after t_* for $\nu \lessapprox .01$. Thus, the last pole to turn around is the first ordered pole β_1, i.e., the one closest to the real axis. For $\nu = 10^{-3}$, the turn-around times for $\beta_j, j = 1, \dots, 4$ are at $t \approx 1.62, 1.51, 1.39, 1.27$, respectively. For $\nu = 10^{-2}$, the turn-around times for $\beta_j, j = 1, \dots, 4$ are at $t \approx 1.05, .55, .425, .325$, respectively. Thus, comparing Figs. 5.13 and 5.15, one can see that the turn-around times $t_u(k)$ increase with decreasing ν. That is, one can relate the time of initial decay of the solution to the turn-around times $t_u(k)$ by comparing the evolution of the poles (see Figs. 5.13, 5.15) to the corresponding evolution of the solution (see Figs. 5.6, 5.16).

Acknowledgment. The author would like to thank the following: Profs. D. Bessis, R. Caflisch, N. Ercolani, J. D. Fournier, L. Greengard, and K. Holczer and Drs. K. Dempsey, L. Cortelezzi, D. Petrasek, H. Rahimizadeh, C. Rippel, and T. Tassa.

REFERENCES

[1] M. J. Ablowitz and H. Segur, *Solitons and the Inverse Scattering Transform*, SIAM, Philadelphia, PA, 1981, pp. 203–209.

[2] M. Abramowitz and I. A. Stegun, *Handbook of Mathematical Functions*, Dover, New York, 1965.

[3] L. V. Ahlfors, *Complex Analysis*, 3rd ed., McGraw-Hill, New York, 1979.

[4] M. Avellaneda, *Statistics of shocks in Burgers turbulence,* II*: Tail probabilities for velocities, shock-strengths and rarefaction intervals*, Comm. Math. Phys., 169 (1995), pp. 45–59.

[5] C. Bardos and S. Benachour, *Domaine d'analyticité des solutions de l'équation d'Euler dans un ouvert de* $\mathbb{R}^n$, Ann. Scuola Norm. Sup. Pisa, 4 (1977), pp. 647–687.
[6] D. Bessis and J. D. Fournier, *Complex singularities and the Riemann surface for the Burgers equation*, Research Reports in Physics: Nonlinear Physics, Springer-Verlag, Berlin, New York, 1990, pp. 252–257.
[7] D. Bessis and J. D. Fournier, *Pole condensation and the Riemann surface associated with a shock in Burgers equation*, J. Phys. Lett., 45 (1984), pp. L833–L841.
[8] R. P. Boas, *Entire Functions*, Academic Press, New York, 1954.
[9] J. M. Burgers, *The Nonlinear Diffusion Equation*, D. Reidel, Boston, MA, 1974.
[10] J. M. Burgers, *A mathematical model illustrating the theory of turbulence*, Adv. Appl. Mech., 1 (1948), pp. 171–199.
[11] R. E. Caflisch, *A simplified version of the abstract Cauchy–Kowalewski theorem with weak singularities*, Bull. Amer. Math. Soc. (N.S.), 23 (1990), pp. 495–500.
[12] R. E. Caflisch, N. Ercolani, T. Y. Hou, and Y. Landis, *Multi-valued solutions and branch point singularities for nonlinear hyperbolic or elliptic systems*, Comm. Pure Appl. Math., 46 (1993), pp. 453–499.
[13] F. Calogero, *Motion of poles and zeros of special solutions of nonlinear and linear partial differential equations and related "solvable" many body problems*, Nuovo Cimento B (11), 43 (1978), pp. 177–241.
[14] J. Carrier, L. Greengard, and V. Rokhlin, *A fast adaptive multipole algorithm for particle simulations*, SIAM J. Sci. and Stat. Comp., 9 (1988), pp. 669–686.
[15] C. Chester, B. Friedman, and F. Ursell, *An extension of the method of steepest descents*, Proc. Cambridge Philos. Soc., 53 (1957), pp. 599–611.
[16] D. V. Choodnovsky and G. V. Choodnovsky, *Pole expansions of nonlinear partial differential equations*, Nuovo Cimento B (11), 40 (1977), pp. 339–353.
[17] J. D. Cole, *On a quasi-linear parabolic equation occurring in aerodynamics*, Quart. Appl. Math., 9 (1951), pp. 225–236.
[18] A. R. Forsyth, *Theory of Differential Equations*, Part IV, Vol. 6, Dover, New York, 1906.
[19] J. D. Fournier and U. Frisch, *L'équation de Burgers deterministe et statistique*, J. Mech. Theory Appl., 2 (1983), pp. 699–750.
[20] U. Frisch and R. Morf, *Intermittency in nonlinear dynamics and singularities at complex times*, Phys. Rev. A (3), 23 (1981), pp. 2673–2705.
[21] L. Greengard and V. Rokhlin, *A fast algorithm for particle simulations*, J. Comp. Phys., 73 (1987), pp. 325–348.
[22] E. Hopf, *The partial differential equation* $u_t + u\,u_x = \mu\,u_{xx}$, Comm. Pure Appl. Math., 3 (1950), pp. 201–230.
[23] N. Joshi and J. A. Petersen, *A method for proving the convergence of the Painlevé expansions of partial differential equations*, Nonlinearity, 7 (1994), pp. 595–602.
[24] D. Kaminski, *Asymptotic expansion of the Pearcey integral near the caustic*, SIAM J. Math. Anal., 20 (1989), pp. 987–1005.
[25] Y. Kimura, *Dynamics of complex singularities for Burgers' equation*, in Proc. NEEDS '94, V. G. Makhankov, ed., World Scientific, Singapore, 1995.
[26] M. D. Kruskal, *The Korteweg–de Vries Equation and Related Evolution Equations*, Lectures in Appl. Math., Amer. Math. Soc., Providence, RI, 1974.
[27] L. Nirenberg, *On the abstract Cauchy–Kowalewski theorem*, J. Differential Geom., 6 (1972), pp. 561–576.
[28] R. B. Paris, *The asymptotic behavior of Pearcey's integral for complex variables*, Proc. Roy. Soc. London Ser. A, 432 (1991), pp. 391–426.
[29] G. Pólya, *Über trigonometrische integrale mit nur reellen nullstellen*, J. Reine Angewandte Math., 158 (1927), pp. 6–18.
[30] Z.-S. She, E. Aurell, and U. Frisch, *The inviscid Burgers equation with initial data of Brownian type*, Comm. Math. Phys., 148 (1992), pp. 623–641.
[31] D. Senouf, *Asymptotic and numerical approximations of the zeros of Fourier integrals*, SIAM J. Math. Anal., 27 (1996), pp. 1102–1128.
[32] D. Senouf, *Dynamics and condensation of complex singularities for Burgers' equation* II, SIAM J. Math. Anal., 28 (1997), pp. 1490–1513.
[33] D. Senouf, R. Caflisch, and N. Ercolani, *Pole dynamics and oscillations for complex Burgers equation in the small dispersion limit*, Nonlinearity, 9 (1996), pp. 1671–1702.
[34] Y. G. Sinai, *Statistics of shocks in solutions of inviscid Burgers equation*, Comm. Math. Phys., 148 (1992), pp. 601–621.
[35] C. Sulem, P. L. Sulem, and H. Frisch, *Tracing complex singularities with spectral methods*,

J. Comp. Phys., 50 (1983), pp. 138–161.
[36] O. Thual, U. Frisch, and M. Hénon, *Application of pole decomposition to an equation governing the dynamics of wrinkled flame fronts*, J. Phys., 46 (1985), pp. 1485–1494.
[37] F. Ursell, *Integrals with a large parameter. Several nearly coincident saddle points*, Proc. Cambridge Philos. Soc., 72 (1972), pp. 49–65.
[38] G. B. Whitham, *Linear and Nonlinear Waves*, Wiley Interscience, New York, 1974.
[39] R. Wong, *Asymptotic Approximations of Integrals*, Academic Press, New York, 1989.